This document is downloaded from the
Digital Open Access Repository of VTT

| | |
|---|---|
| Title | Hydrogen enhancement potential of synthetic biofuels manufacture in the European context: A techno-economic assessment |
| Author(s) | Hannula, Ilkka |
| Citation | Energy. Elsevier Ltd . Vol. 104 (2016) No: June, Pages 199-212 |
| Date | 2016 |
| URL | DOI: 10.1016/j.energy.2016.03.119 |
| Rights | This preprint article may be downloaded for personal use only. |

VTT
http://www.vtt.fi
P.O. box 1000
FI-02044 VTT
Finland

By using VTT Digital Open Access Repository you are bound by the following Terms & Conditions.

I have read and I understand the following statement:

This document is protected by copyright and other intellectual property rights, and duplication or sale of all or part of any of this document is not permitted, except duplication for research use or educational purposes in electronic or print form. You must obtain permission for any other use. Electronic or print copies may not be offered for sale.

# Hydrogen enhancement potential of synthetic biofuels manufacture in the European context: A techno-economic assessment

Ilkka Hannula[1]

*VTT Technical Research Centre of Finland Ltd, P.O. Box 1000, FI-02044 VTT, Finland*

**Abstract**

Potential to increase biofuels output from a gasification-based biorefinery using external hydrogen supply (enhancement) was investigated. Up to 2.6 or 3.1-fold increase in biofuel output could be attained for gasoline or methane production over reference plant configurations, respectively. Such enhanced process designs become economically attractive over non-enhanced designs when the average cost of low-carbon hydrogen falls below 2.2 - 2.8 €/kg, depending on the process configuration. If all sustainably available wastes and residues in the European Union (197 Mt/a) were collected and converted only to biofuels, using maximal hydrogen enhancement, the daily production would amount to 1.8 - 2.8 million oil equivalent barrels. This total supply of hydrogen enhanced biofuels could displace up to 41 - 63 per cent of the EU's road transport fuel demand in 2030, again depending on the choice of process design.

*Keywords:* Biomass residues, Gasification, Electrolysis, Carbon dioxide, Synthetic fuels, European Union

## 1. Background

The amount of atmospheric carbon is currently increasing at a rate of 4.3 ± 0.1 gigatonnes (C) per year, mainly as a result of human activity [1]. Multiple lines of scientific evidence show that this increasing amount of carbon in the atmosphere is warming the global climate system [2, 3, 4]. To limit warming under 2 °C, the European Council in 2011 reconfirmed the EU objective of reducing greenhouse gas (GHG) emissions by 80-95 % by 2050 compared to 1990. The European Council also endorsed a binding EU target of at least 40 % domestic reduction in GHG emissions by 2030 compared to 1990. The target will be achieved collectively by the EU in the most cost-effective manner possible, with the reductions in the ETS and non-ETS sectors amounting to 43 % and 30 % by 2030 compared to 2005, respectively.

Although carbon emissions are generally falling in the European Union, transportation still counts among the few sectors that resist this overall trend (see Fig. 1), as the

*Email address:* ilkka.hannula@vtt.fi ()

[1]Telephone: +358 20 722 6370

progress made in improving vehicle efficiency has been largely off-set by the increased amount of personal and freight transport. Therefore, a wide-ranging switch to renewable fuels is required for driving down transportation emissions in the long term. According to an IEA roadmap study [5], biofuels (i.e. fuels produced from renewable plant matter) could provide 27 % of total transport fuel consumption by 2050 while avoiding around 2.1 gigatonnes of $CO_2$ emissions per year if sustainably produced. However, meeting this demand would require 65 exajoules of biofuel feedstock, occupying around 100 million hectares of land, which was considered challenging by the study given the growing competition for land for food and fibre.

Table 1: Present and future (2030) availability of sustainable wastes and residues in the EU [6].

| Category | Subcategory | Current availability, Mt/a | 2030 availability, Mt/a |
|---|---|---|---|
| Waste | Paper | 17.5 | 12.3 |
| | Wood | 8 | 5.6 |
| | Food and garden | 37.6 | 26.3 |
| Crop residues | | 122 | 139 |
| Forestry residues | | 40 | 40 |
| | Sum | 225 | 223 |

Searle and Malins [6] examined the availability of wastes and residues in the European Union that might be realistically mobilised in an economically viable manner for the production of advanced biofuels. Their estimates on the present and future (2030) feedstock availabilities in different categories is shown in Table 1. According to their findings, almost 1 million oil equivalent barrels per day could be supplied based on these feedstocks, displacing 16 per cent of road transport fuel demand in 2030 [6]. However, it is likely that competition over feedstocks will restrict the total potential, so the estimate should be understood as upper limit for the biofuels supply.

## 2. Introduction

This paper examines the potential to increase fuels production from a given amount of biomass, by feeding additional hydrogen to a gasification-based biorefinery. The process is not sensitive to the origin of the hydrogen, but production via electrolysis of water, driven by electricity from low-carbon sources like wind, solar, hydropower or nuclear[2] is examined as a possible option. The investigation is based on a systematic analysis and comparison of eight selected plant configurations capable of producing synthetic biofuels from biomass feedstocks via thermochemical gasification. Mass and energy flows are calculated for each plant configuration with ASPEN® Plus (Aspen) process simulation software. The overall economics are also evaluated in terms of euros (€) per gigajoule (GJ), from the perspective of a synthetic fuel producer, based on an underlying component-level capital cost estimates.

[2]Biomass is also an important source of low-carbon electricity, but this option is excluded here as it would compete for the same resource.

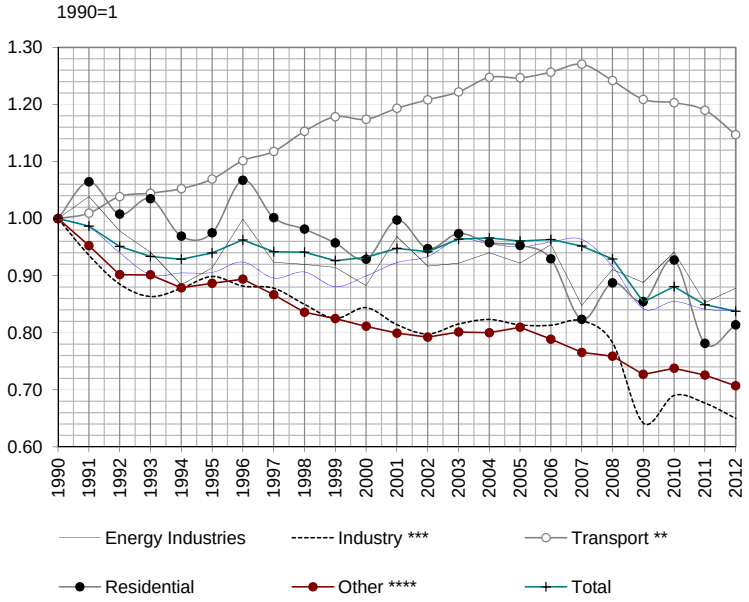


Figure 1: GHG emissions* by sector in EU-28. Million tonnes $CO_2$ equivalent. (*) Excluding LULUCF (Land Use, Land-Use Change and Forestry) emissions and International Bunkers; (**) Excluding International Bunkers (international traffic departing from the EU); (***) Emissions from Manufacturing and Construction and Industrial Processes; (****) Emissions from Fuel Combustion in Agriculture/Forestry/Fisheries, Other (not specified elsewhere), Fugitive Emissions from Fuels, Solvent and Other Product Use, Agriculture, Waste, Other. [7].

The production of synthetic fuels (synfuels) from carbonaceous feedstocks is a well-established technology, although all commercial scale plants to date have been operated with fossil feedstocks (such as coal and natural gas) and redesign of some key parts of the process is required to switch using renewable feedstocks. A considerable amount of work has been done to accelerate the progress of synthetic biofuels technologies [8], which are currently moving through research, development and demonstration to commercialisation [9, 10, 11, 12].

The possibility to enhance synthetic biofuels production with additional (electrolytic) hydrogen has been occasionally discussed in the scientific literature. Mignard and Pritchard [13] noted, using methanol production as an example, that the integration can contribute to more effective utilisation of biomass by increasing the methanol output by 130 %. They also noted that co-utilisation of biomass and electricity could rise to prominence in the future if competition over land availability with food and feed production starts to limit the contribution of biofuels to a low-carbon economy. Hansen et al. [14] studied the consequences of using solid oxide electrolysis (SOEC) to assist methanol production from biomass gasification and concluded that methanol production can be more than doubled at the expense of using significant amount of electricity to drive the electrolysis. Pozzo et al. [15] analysed an advanced concept where dimethyl ether (DME) was produced with biomass gasification and high-temperature co-electrolysis (SOEC). They noted that the specific productivity of DME from biomass could be greatly increased (nearly doubled) by electrolyser enhancement. Hannula [16] examined the impact of a slight hydrogen addition on the performance and costs of synfuels production and found hydrogen supplemented biofuels more cost-effective than non-biomass synfuels (electrofuels) under a wide range of economic assumptions.

## 3. Methods

### *3.1. Plant configurations*

All plant configurations analysed in this work are based on a thermochemical conversion of biomass residues to synthesis gas via gasification, followed by subsequent catalytic conversion of synthesis gas to fuels. These *base case* process configurations are compared with *enhanced* process configurations where biomass-derived synthesis gas is supplemented with external hydrogen to maximise the conversion of synthesis gas carbon to fuel. The considered plant configurations illustrate two basic gasification alternatives:

- autothermal (direct) gasification with a mixture of steam and oxygen, or
- allothermal (indirect) gasification with steam;

and two different end-product alternatives:

- synthetic gasoline via methanol, or
- synthetic natural gas (methane).

In addition, following alternatives for the treatment of syngas $CO_2$ are examined:

- removal by a physical scrubbing system,

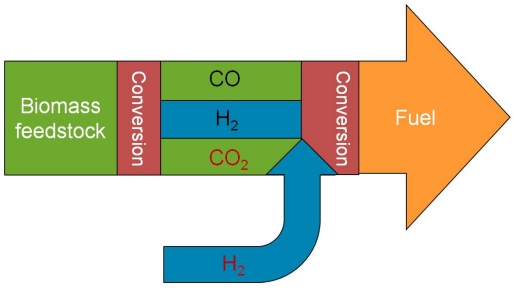


Figure 2: Schematic representation of a hydrogen-enhanced gasification-based biorefinery process concept evaluated in this work.

Table 2: Summary of examined plant configurations.

| Configurations | Gasifier type | Stoichiometry adjusted by | $CO_2$ removal | Electrolyser | ASU* | End product |
|---|---|---|---|---|---|---|
| OG | $O_2$ | Sour shift | Yes | | Yes | Gasoline |
| OG+ | $O_2$ | $H_2$ addition | | Yes | | Gasoline |
| OM | $O_2$ | Sour shift | Yes | | Yes | Methane |
| OM+ | $O_2$ | $H_2$ addition | | Yes | | Methane |
| SG | Steam | Gasifier | Yes | | Yes | Gasoline |
| SG+ | Steam | $H_2$ addition | | Yes | | Gasoline |
| SM | Steam | Gasifier | Yes | | Yes | Methane |
| SM+ | Steam | $H_2$ addition | | Yes | | Methane |

*ASU = cryogenic Air Separation Unit.

- conversion to fuel with additional hydrogen from external source.

The combination of these alternatives gives eight basic configurations, each characterised by distinctive plant designs. The plants are identified by a sequence of two letters, where first letter indicates the gasifier type (O = oxygen, S = steam) and second letter the main product (G = gasoline, M = methane). In addition, for plant configurations that feature external hydrogen supply (to maximise overall carbon conversion), the acronyms are amended with a plus (+) sign. For a summary of the examined alternatives, see Table 2. A schematic illustration of the enhanced plant designs is given in Fig. 2, while process layouts (excluding syntheses) are given in Figs. A.10, A.11, A.12 and A.13. The following paragraphs provide brief technology overviews that are complemented with a list of main simulation parameters in Table B.8. For a more detailed discussion on component technologies and modelling approaches, please refer to the online supplement.

### *3.1.1. Biomass to synthesis gas*

Forest residue chips are considered as feedstock for all examined plant designs. The chips are produced from residue formed during harvesting of industrial wood and thus includes needles and has a higher proportion of bark than chips made out of whole trees [17]. The higher heating value (HHV) of the dry matter is 20.67 MJ/kg and the lower heating value (LHV) is 19.34 MJ/kg. Additional feedstock properties are described in Table 3.

The wet biomass feedstock (stream 1 in process layouts) is first dried from its initial moisture of 50 wt% to 15 wt% with a belt dryer and fed (stream 7) to a fluidised-bed

Table 3: Properties of the gasifier feedstock [17].

| | |
|---|---|
| **Proximate analysis, wt% d.b.*** | |
| Fixed carbon | 25.3 |
| Volatile matter | 70.8 |
| Ash | 3.9 |
| **Ultimate analysis, wt% d.b.** | |
| Ash | 3.9 |
| C | 53.2 |
| H | 5.5 |
| N | 0.3 |
| Cl | 0 |
| S | 0.04 |
| O (difference) | 37.06 |
| **Other properties** | |
| HHV, MJ/kg | 20.67 |
| LHV, MJ/kg | 19.34 |
| Bulk density, kg d.b./$m^3$** | 293 |
| Sintering temp. of ash, °C | >1000 |

*wt% d.b. = weight percent dry basis
**1 litre batch, not shaken

gasification reactor operated either with a mixture of steam and oxygen (autothermal gasifier configurations: OG, OG+, OM and OM+) or steam (allothermal gasifier configurations: SG, SG+, SM and SM+). During gasification, the wood residue chips are converted to raw product gas containing CO, $H_2$, $CO_2$, $H_2O$, $CH_4$, small amount of higher hydrocarbons and tars [18]. The gasifier effluent (stream 10) is cooled down (by heat exchanger HX-C1 that recovers sensible heat for water evaporation) to 550 °C to facilitate the removal of entrained dust by a ceramic filter [19]. The gas then enters a catalytic reformer where tars and hydrocarbons are converted to light gases [20]. For plants that produce gasoline (OG, OG+, SG and SG+) the tar reformer is designed for maximal methane[3] conversion (95 % at 950 $°C_{exit}$), while for plants that produce synthetic natural gas (OM, OM+, SM, SM+) methane conversion is minimised (35 % at 850 $°C_{exit}$). The simulation model for the gasifier-filter-reformer combination is validated with experimental data derived from a 0.5 $MW_{th}$ process development unit (PDU) run circa 4000 hours in pressurised oxygen-blown mode using various wood residues as feedstock [21]. The model itself is described in detail in Refs. [22, 23].

The reformed tar-less gas (12) is cooled (superheater HX-C2 and boiler HX-C3) down to 200 °C, while recovering sensible heat for the production of superheated steam. For base case configurations that feature oxygen gasification (OG and OM in Fig. A.10) the syngas modulus ($H_2$/CO ratio) is adjusted by an adiabatic sour shift reactor between the cooling steps, while for other base case configurations the stoichiometric requirements are achieved already during steam gasification[4]. In the enhanced configurations the

[3]This refers to methane that is unavoidably formed during biomass gasification.
[4]In the SM configuration some $CO_2$ needs to be fed along with steam to the gasifier to reach a correct

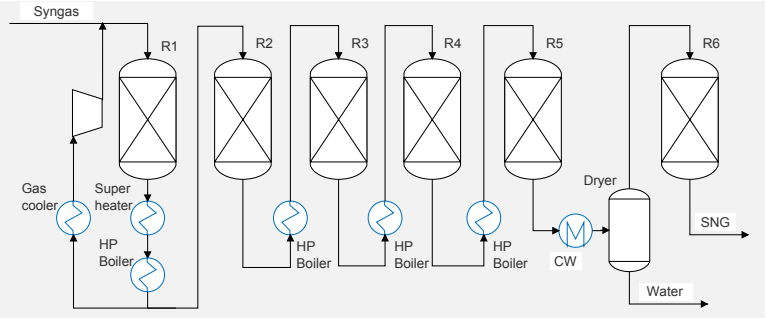


Figure 3: Layout for the high temperature methanation section.

stoichiometry is controlled by external hydrogen addition (19) from an electrolyser. The 200 °C gas (13) is fed to a two-stage water scrubber where it cools down to 60 °C while recovering sensible heat for feedstock drying and district heating. Finally, the gas is cooled down to 30 °C to remove syngas moisture. The dried gas (15) is then compressed and cooled down (HX-C6) to enable efficient removal of acid gases (from stream 16) using acid gas removal (AGR) unit operated with chilled methanol as washing solvent. In the base case configurations the AGR is used to remove both $CO_2$ and sulphur species from the syngas, while in the enhanced configurations only sulphur is removed (as $CO_2$ is used as feedstock for the synthesis). The additional hydrogen is produced via low temperature alkaline water electrolyser. The purity of the electrolytic hydrogen and oxygen is assumed to be 100 % due to very low concentration of contaminants in the demineralised tap water used as feedstock [24]. In the enhanced configurations, byproduct oxygen from water electrolysis is utilised for the biomass conversion process (for oxygen gasification and/or reforming), while in the base case configurations a dedicated cryogenic oxygen plant (Air Separation Unit, ASU) is required. System efficiency of the alkaline electrolyser, defined as hydrogen output (LHV) divided by electrical energy input to the electrolyser system, is set to 67 %. Before the catalytic synthesis, syngas is treated by guard beds that remove possible remnants of sulphur downstream from the AGR.

For plants that produce methane (SNG), syngas is compressed to 1.6 MPa at one go.[5] For gasoline configurations, syngas is compressed to 8.0 MPa in two steps: to 2.1 MPa before acid gas removal followed by further compression to 8.0 MPa, the operating pressure of methanol converter.

### *3.1.2. Synthesis of methane*

Hydrogenation of carbon oxides to methane over nickel catalyst can be described [25, 26] with the following reactions:

$$CO + 3H_2 = CH_4 + H_2O \quad \Delta H = -206 \text{ kJ/mol}, \tag{1}$$

$$CO_2 + 4H_2 = CH_4 + 2H_2O \quad \Delta H = -165 \text{ kJ/mol}. \tag{2}$$

modulus for the methanol synthesis.

[5]This allows for 0.1 MPa pressure drop in the AGR as inlet pressure to methanation is 1.5 MPa.

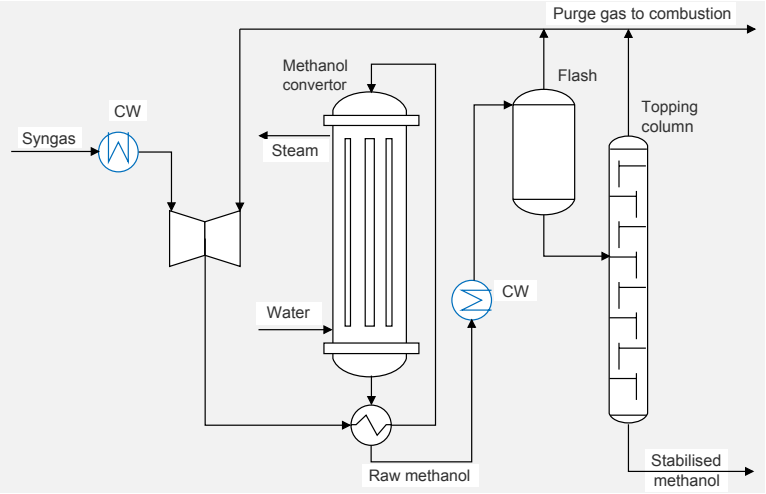


Figure 4: Layout for the low-pressure methanol synthesis section.

The methanation process design adopted for this work features six adiabatic fixed-bed reactors connected in series and equipped with intercoolers (See Fig. 3 for layout). The pressure at the inlet of the first reactor is 1.5 MPa. The inlet syngas is mixed with recycle gas and preheated to 300 °C. The amount of recycling is chosen to limit temperature increase in the first reactor to 700 °C. The hot effluent exiting from the first four reactors is cooled to 300 °C before entering the next reactor in series. Effluent from the fifth reactor is cooled down to condense and separate gas moisture before feeding to the last reactor. Overall extent of syngas conversion to methane is >99.5 % and the effluent exits from the system at 1.1 MPa pressure. The recovered heat is used to produce high pressure superheated steam for the steam cycle of the gasification plant.

*3.1.3. Synthesis of methanol*

Hydrogenation of carbon oxides to methanol over copper oxide catalyst can be described [27, 28] with the following reactions:

$$CO_2 + 3H_2 = CH_3OH + H_2O \; \Delta H = -40.9 \text{ kJ/mol}, \tag{3}$$

$$CO + 2H_2 = CH_3OH \; \Delta H = -90.7 \text{ kJ/mol}. \tag{4}$$

As both reactions are exothermic and accompanied by net decrease in molar volume, the equilibrium is favoured by high pressure and low temperature. The methanol synthesis design adopted for this work features a tubular boiling-water reactor operated at 260 °C and 8.0 MPa (see Fig. 4 for layout). The fresh synthesis gas feed is admixed with a recycle stream and preheated to 260 °C in heat exchange with the hot reactor effluent. Any unconverted synthesis gas is separated from the effluent at the reactor exit, and recirculated back to the feed side of the reactor until 95 % conversion of CO, $CO_2$ and $H_2$ to methanol is achieved. Small amount of unconverted gas is continuously purged to control the build-up of inerts in the methanol loop, followed by combustion in the

oxidiser.

The produced raw methanol contains mainly dissolved gases and reaction water formed as byproduct of $CO_2$ conversion. The dissolved gases are removed in a stabilising column, but water is left in the solution to facilitate subsequent conversion of raw methanol to gasoline.

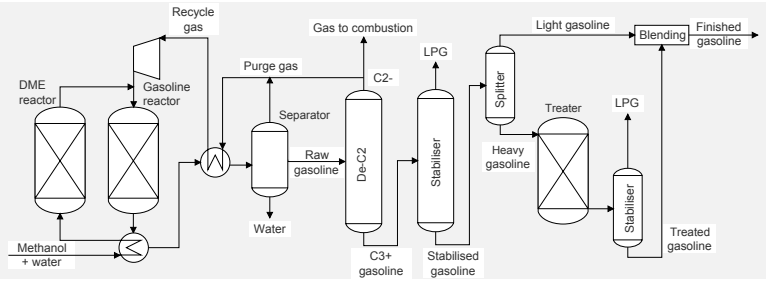


Figure 5: Layout for the two-step methanol-to-gasoline synthesis section.

### *3.1.4. Synthesis of gasoline*

The conversion of methanol to gasoline proceeds essentially according to reaction

$$nCH_3OH \rightarrow (CH_2)_n + nH_2O, \tag{5}$$

where $(CH_2)_n$ represents a wide range of paraffinic and aromatic hydrocarbons produced in the gasoline synthesis step [29]. The process, called methanol-to-gasoline (MTG), features an adiabatic dehydration and gasoline reactor in series (see Fig. 5 for layout). The methanol feed is pumped to 2.27 MPa followed by vaporisation and superheating to 297 °C in heat exchange with the hot reactor effluent. An adiabatic fixed-bed dehydration reactor is used to convert the feed to an equilibrium mixture of methanol, DME and water. The effluent exits the reactor at 407 °C and 2.17 MPa, is admixed with recycle gas and fed to a second reactor where it is converted to gasoline [30]. A recycle stream is used to limit the outlet temperature of the adiabatic gasoline reactor to 400 °C. To control the build-up of inerts in the synthesis loop some gas is continuously purged from the recycle flow and transferred to combustion. The gasoline reactor effluent is condensed and separated into water, raw gasoline, purge and recycle gas streams. The raw gasoline is then fractionated by distillation to produce finished gasoline blendstock containing less than 2 wt% durene together with a byproduct stream resembling liquefied petroleum gas (LPG) [31, 32]. It is assumed that the recovery of waste heat provides the needed utilities for the upgrading, leading to zero net parasitic utilities demand for the area.

Post-processing of methanol into gasoline (MTG synthesis) can take place either at the same site with methanol production, or at a different site preferably integrated with a petroleum refinery. The latter approach would allow a two-step production concept featuring decentralised production of methanol at several sites close to biomass resources, followed by centralised MTG conversion at a large-scale plant allowing economies of scale for the second step of the conversion pathway. As a result, purge gas flows from the MTG

plant are reported separately (i.e. not combusted at the gasification plant) in the results table and considered as a separate saleable commodity in the cost analysis.

### *3.2. Performance analysis*

The performance analysis rests on mass and energy flows calculated with ASPEN Plus® (Aspen) process simulation software. Following metrics are calculated to assist the investigation:

First-law efficiency from biomass and electricity to synfuel

$$\eta_{overall} = \frac{(\dot{m} * H)_{\text{synfuel}}}{(\dot{m} * H)_{\text{wet biomass}} + electricity}, \tag{6}$$

where $\dot{m}$ represents mass flow (kg/s), $H$ lower heating value (MJ/kg), and *electricity* the electrolyser work input ($MW_e$) required to produce additional hydrogen for enhanced configurations;

First-law efficiency from electricity to added synfuel

$$\eta_{electricity} = \frac{\Delta(\dot{m} * H)_{\text{synfuel}}}{electricity}, \tag{7}$$

where $\Delta(\dot{m}*H)_{\text{synfuel}}$ refers to the additional amount of synfuel produced by enhanced configurations in relation to comparable non-enhanced configuration;

Overall carbon conversion

$$\eta_{carbon} = \frac{\dot{n}_{\text{carbon in synfuel}}}{\dot{n}_{\text{carbon in biomass}}}, \tag{8}$$

where $\dot{n}$ denotes mole flow (kmol/s); and

Mass yield

$$\text{Yield}_{\text{mass}} = \frac{\dot{m}_{\text{synfuel}}}{\dot{m}_{\text{dry biomass}}}. \tag{9}$$

All the examined plant configurations have been designed self-sufficient in terms of heat and steam, while electricity is balanced with the electric grid. In all calculations lower heating value for biomass at 50 wt% moisture is used.

### *3.3. Cost analysis*

The overall economics are evaluated in terms of euros (€) per gigajoule (GJ), based on an underlying component-level capital cost estimates. The investment cost estimates are based on a self-consistent set of component-level capital cost data assembled using literature sources, vendor quotes and discussions with industry experts. A detailed summary of the equipment cost database is available in the online supplement. All equipment costs have been escalated to correspond with 2010 euros using *Chemical Engineering* magazine's Plant Cost Index[6] to account for inflation. Individual cost scaling exponents ($k$)

[6]For more information, see: www.chemengonline.com/pci.

have been used to scale the reference capital costs ($C_o$) to a capacity that corresponds with simulation results ($S$) using the following relation:

$$C = C_0 \times \left(\frac{S}{S_0}\right)^k, \tag{10}$$

where $S_0$ is the scale of reference equipment and $C$ the cost of equipment at the size suggested by the simulation.

Total plant cost (TPC) is defined as the "overnight" capital investment required to construct a plant and includes all main equipment (with initial catalyst loadings) plus installation (labour), indirect costs (engineering and fees), project contingency and (in some instances) unscheduled equipment. These cost items are reported as fractions from the (installed) equipment costs. The total capital investment (TCI) is then obtained by adding interest during construction to TPC. The estimates are assumed to carry an accuracy of -15%/+30%, which is typical for studies based on prefeasibility level factored approach [33].

The annual capital charges are calculated from the TCI using 0.12 capital charge rate based on 10 % weighted average cost of capital (WACC) and 20-year economic life for the biorefinery. The yearly operating and maintenance (O&M) costs[7] are assumed to be 4 % of the TPC [34] and plants are expected to run 8000 hours per year (91 % availability factor). Biomass is valued at 5 €/GJ (18 €/MWh)[8], byproduct district heat at 11 €/GJ (∼40 €/MWh) and electricity at 14 €/MWh (∼50 €/MWh). Surplus oxygen from the electrolyser (after on-site consumption) is vented to atmosphere, not sold.

The levelised cost of fuel (LCOF) production is evaluated according to the following equation:

$$LCOF(€/GJ) = \frac{F + E + C + O - R}{P}, \tag{11}$$

where

- $F$ is the annual cost of biomass residues,
- $E$ is the annual cost of electricity,
- $C$ is the annualised capital charge, including return on equity and interest on debt,
- $O$ is the annual operating and maintenance costs, and
- $R$ is the annual revenue from selling by-products (district heat, purge gas and LPG).[9]

The sum of these annual costs (€/a) is divided by $P$, which is the annual output of fuel (GJ/a) from the plants. When defined in this way, LCOF (€/GJ) indicates the product sale price needed to break-even under the technical and economic parameters assumed.

[7] Following breakdown is assumed for the O&M: Personnel costs 0.5 %, Maintenance & insurances 2.5 %, Catalysts & chemicals 1 %.

[8] Price for forest residues (thinnings, stumps and slash) and industry byproduct (sawdust and bark) traded for energy or heat production purposes in Finland. Source: FOEX Indexes Ltd.

[9] Purge gas and LPG are only sold from plant designs that feature gasoline synthesis.

Table 4: Financial parameters employed in the cost analysis.

| | |
|---|---|
| **Financial parameters** | |
| Economic life for plant | 20 years |
| WACC* (discount rate) | 10 % |
| Capital charge rate | 0.1175 |
| Annual O&M cost factor | 4 %** |
| Annual operating hours | 8000 |
| Interest during construction | 5 %*** |
| Investment support, M€ | 0 |
| **Values of inputs/outputs** | |
| Biomass residue chips, €/GJ | 5 |
| Electricity, €/GJ | 14 |
| District heat, €/GJ | 11 |
| Fuel gas, €/GJ | 10 |
| LPG, €/GJ | 12 |
| Water, €/t | 0 |

*Weighted Average Cost of Capital
**Fraction of Total Plant Cost
***Fraction of Total Capital Investment

## 4. Results

Mass and energy flows have been simulated for all examined plant configurations. All plants consume 100 MW (LHV) of wet (50 wt%) biomass residues, corresponding to 5.92 kg/s flow of dry biomass into the process. The results are summarised in Table B.9 and additionally visualised for the enhanced plant configurations in Figs. 6 and 7. With non-enhanced plant configurations 51.8 MW of gasoline or 66.8 MW of methane can be produced via oxygen gasification. For steam gasification the gasoline output is 51.0 MW and methane output to 63.7 MW. When syngas $CO_2$ is also converted to fuels using additional hydrogen supply, the gasoline output increases to 134.0 MW (oxygen gasification) or to 98.0 MW (steam gasification), while methane output is increased to 205.4 MW (oxygen gasification) or 139.9 MW (steam gasification).

The calculated performance metrics have been summarised in Table 5. The highest $\eta_{overall}$ is attained by non-enhanced methane production via oxygen gasification (66.8 %, OM) and the lowest by enhanced gasoline production via oxygen gasification (49.7 %, OG+). The addition of electrical input to the process contributes to additional synfuel produced. With the state-of-the-art alkaline electrolyser technology chosen for this work, 48.4 to 55.1 % energy conversion efficiencies from electricity to synfuel (LHV) can be achieved. Mass yields lay in the range of 193 to 226 kg/tonne$_{\text{dry biomass}}$ for the non-enhanced configurations but can be dramatically increased up to 694 kg/tonne$_{\text{dry biomass}}$ with maximal hydrogen enhancement.

### *4.1. Carbon and energy flows*

The carbon flows are visualised for the enhanced plant configurations in Fig. 8. Although the cold gas efficiencies of the autothermal (oxygen) and allothermal (steam)

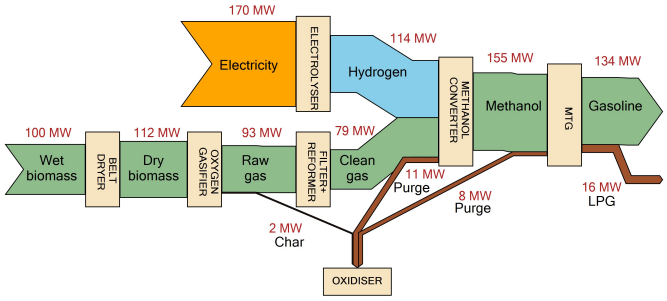


(a) Gasoline via oxygen gasification (OG+).

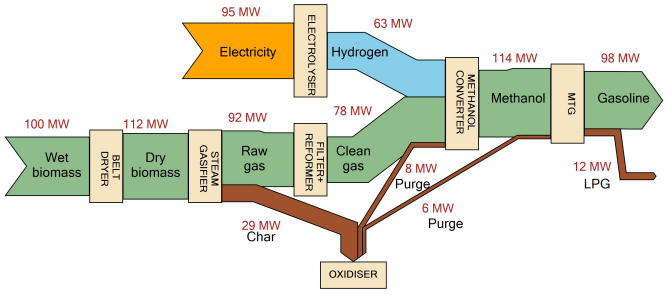


(b) Gasoline via steam gasification (SG+).

Figure 6: Simulated energy flows for gasoline configurations featuring hydrogen enhancement.

Table 5: Performance metrics for the examined plant configurations.

| **Configuration** | | OG | OG+ | OM | OM+ | SG | SG+ | SM | SM+ |
|---|---|---|---|---|---|---|---|---|---|
| $\eta_{overall}$ | % | 51.8 | 49.7 | 66.8 | 58.4 | 51.0 | 50.3 | 63.7 | 58.7 |
| $\eta_{electricity}$ | % | | 48.4 | | 55.1 | | 49.7 | | 55.0 |
| $\eta_{carbon}$ | % | 30.5 | 79.4 | 32.5 | 98.0 | 28.8 | 58.4 | 31.4 | 67.0 |
| $\text{Yield}_{\text{mass}}$ | kg/tonne | 196 | 507 | 226 | 694 | 193 | 370 | 215 | 473 |

gasifiers are fairly similar, their carbon flows are very different, and tracing the flow of carbon through the plants reveal useful insights into the examined designs.

In oxygen gasification - where heat is generated within the gasifier by partial oxidation - all $CO_2$ leaves the gasifier from a single exit as synthesis gas, whereas in steam gasification - where oxidation reactions take place in a separate reactor with air - part of the $CO_2$ "escapes" further processing as nitrogen-diluted flue gas (for more discussion, please refer to the supplement).

The second significant difference in carbon flows relate to the way syntheses operate. In methane production, all compounds in the fresh syngas feed end up in the product (with the exception of reaction water that is removed by means of condensation), while in methanol and gasoline production a stream of purge gas is removed from the recycle

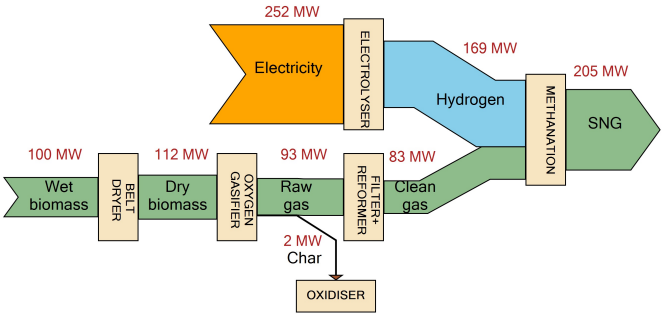


(a) Methane via oxygen gasification (OM+).

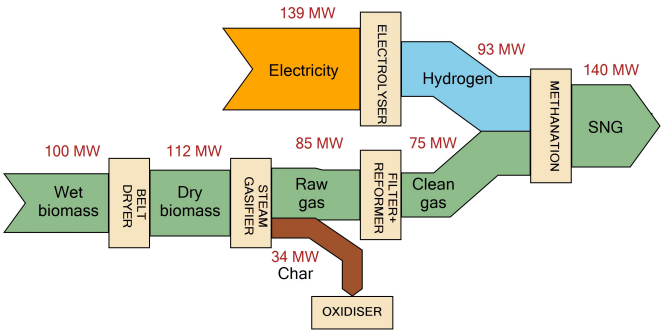


(b) Methane via steam gasification (SM+).

Figure 7: Simulated energy flows for methane (SNG) configurations featuring hydrogen enhancement.

loop[10] to avoid build-up of inerts in the system. Some carbon is thus inevitably lost from the process, contributing to lower overall carbon conversion $\eta_{carbon}$.

The implications of these features are also quantified in Table 5. The overall carbon conversions of base case plant designs range from 28.8 % to 32.5 % the lowest being for gasoline production via steam gasification and the highest for methane (SNG) production via oxygen gasification, as expected based on the discussion above. For the enhanced configurations, carbon conversions range from 58.4 % to 98.0 % the lowest being again for gasoline production via steam gasification and the highest for methane production via oxygen gasification. So the difference in overall carbon conversion between the lowest and highest configurations is a remarkable 69.2 percentage points.

### *4.2. Process economics*

The Total Capital Investment (TCI) estimates for the examined plant configurations, excluding equipment needed for external hydrogen generation, are given in Table B.10. The TCIs range from 173 to 272 M€. The TCIs for plant configurations that feature steam gasification are estimated to have 7 - 22 M€ lower TCI than corresponding plants featuring oxygen gasification. These reductions are caused by the lack of - or reduced

[10]Purge gas is combusted in the oxidiser, thus allowing carbon to exit the process as nitrogen-diluted flue gas.

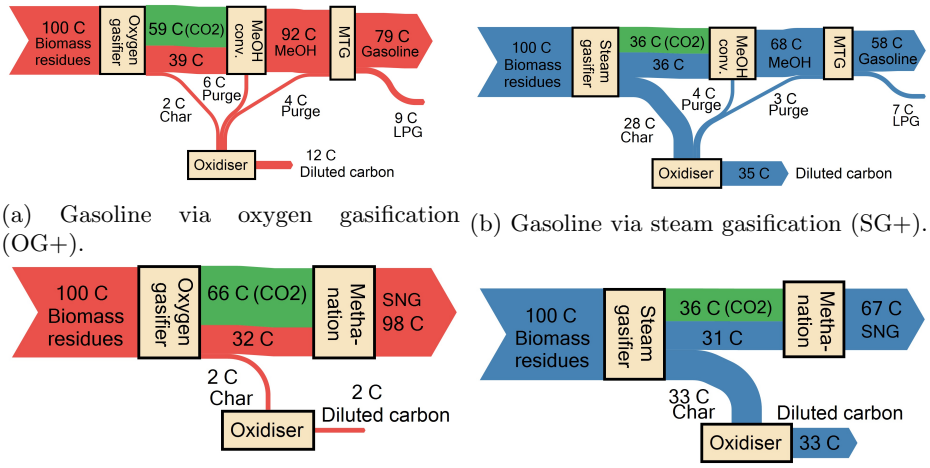


(a) Gasoline via oxygen gasification (OG+).

(b) Gasoline via steam gasification (SG+).

(c) Methane via oxygen gasification (OM+).

(d) Methane via steam gasification (SM+).

Figure 8: Simulated carbon flows for configurations that feature hydrogen enhancement. The green coloured flow is the amount of carbon that in the non-enhanced configurations is separated by AGR and vented to atmosphere.

need for - oxygen, water-gas shifting and $CO_2$ removal (where applicable). The enhanced configurations have higher TCIs than the comparable base case designs, which is explained by the greatly enlarged synthesis sections of the enhanced configurations that off-set the reduced investments in $CO_2$ removal and oxygen production.[11] For all configurations, methane-producing plants feature the lowest TCIs, ranging from 173 to 190 M€, while for gasoline-producing plants the TCIs range from 227 to 272 M€.

The levelised cost of fuel (LCOF) production for the examined plant configurations is calculated in Table 6 using cost parameters given in Table 4. The LCOFs range from 20.4 to 31.3 €/GJ among the cases analysed. In Table 6 the cost of hydrogen addition has been set to a level that yields the same LCOF than for the comparable enhanced and base case configurations. For example, the base case gasoline plant featuring oxygen gasification (OG) has a LCOF of 31.3 €/GJ and for the enhanced configuration to achieve the same LCOF, the levelised cost of renewable hydrogen should be 22.9 €/GJ (82.6 €/MWh or 2.8 €/kg). If low-carbon hydrogen can be purchased at a lower cost than this break-even price, enhanced configuration will become more profitable than the comparable non-enhanced plant.

The corresponding break-even electricity prices are also calculated[12] for the Table. For gasoline configurations, hydrogen enhancement becomes feasible when the average annual cost of electricity drops below 35.4 €/MWh (OG+) or 33.9 €/MWh (SG+).

[11] For all enhanced configurations, byproduct oxygen output from the electrolyser greatly exceeds on-site demand by the biomass conversion process, making it possible to drop the investment for a dedicated air separation unit.

[12] Assuming 1 €/$W_e$ specific investment cost for the alkaline electrolyser system, 67 % system efficiency (LHV), 8000 hours annual operating time, 0.12 capital charge rate and annual O&M cost as 4 % of the electrolyser investment.

Table 6: Breakdown of LCOFs under economic assumptions summarised in Table 4. The cost of hydrogen has been set to a level that gives same levelised production cost for the comparable enhanced and non-enhanced plant configuration.

| **Configuration** | OG | OG+ | OM | OM+ | SG | SG+ | SM | SM+ | |
|---|---|---|---|---|---|---|---|---|---|
| Biomass residues (at 5 €/GJ) | 14.4 | 14.4 | 14.4 | 14.4 | 14.4 | 14.4 | 14.4 | 14.4 | M€/a |
| O&M (at 4 % of TPC/a) | 8.9 | 10.4 | 6.9 | 7.2 | 8.7 | 9.5 | 6.6 | 6.9 | M€/a |
| Capital charges (at 0.12 ccr) | 27.5 | 31.9 | 21.4 | 22.3 | 26.7 | 29.4 | 20.3 | 21.2 | M€/a |
| Electricity (at 14 €/GJ)* | 1.7 | 3.1 | 0.3 | -3.0 | 1.0 | 2.0 | -0.9 | -2.6 | M€/a |
| District heat (at 11 €/GJ) | -2.8 | -6.5 | -1.9 | -10.2 | -3.2 | -4.7 | -3.0 | -7.5 | M€/a |
| MTG fuel gas (at 10 €/GJ) | -0.9 | -2.2 | | | -0.9 | -1.6 | | | M€/a |
| MTG LPG (at 12 €/GJ) | -2.1 | -5.5 | | | -2.1 | -4.0 | | | M€/a |
| External hydrogen purchases | | 75.1 | | 95.8 | | 40.6 | | 49.9 | M€/a |
| Total annual costs | 46.7 | 120.7 | 41.2 | 126.6 | 44.6 | 85.6 | 37.4 | 82.2 | M€/a |
| Levelised production cost | 31.3 | 31.3 | 21.4 | 21.4 | 30.4 | 30.4 | 20.4 | 20.4 | €/GJ |
| Break-even hydrogen price | | 22.9 | | 19.7 | | 22.3 | | 18.7 | €/GJ |
| | | 82.6 | | 71.1 | | 80.4 | | 67.3 | €/MWh |
| | | 2.8 | | 2.4 | | 2.7 | | 2.2 | €/kg |
| Break-even electricity price | | 35.4 | | 27.7 | | 33.9 | | 25.1 | €/MWh |

*Electricity used for hydrogen production not included here.

For methane configurations the break-even thresholds are 27.7 €/MWh (OM+) or 25.1 €/MWh (SM+). The relatively high production cost estimates for the non-enhanced configurations in Table 6 are a consequence of the fairly small size of the analysed plants (100 $MW_{th}$ biomass input) that prevents benefits through economies of scale.

Finally, the impact of electricity price on the production cost of synthetic gasoline is investigated in Fig. 9, where break-even oil price[13] for OG+ configuration is illustrated at three biomass price[14] levels: 30 €/t, 55€/t and 80 €/t (or 7.7 €/MWh, 14.1 €/MWh and 20.6 €/MWh, assuming 14 GJ/t for biomass residues at 15 wt% moisture). For zero cost electricity - representing naturally the lowest cost scenario - the break-even oil price would be from 85 to 102 $/barrel depending on the cost of biomass.

## 5. Discussion

A comprehensive analysis on the performance and costs of plants producing synthetic fuels from biomass residues or from biomass residues and electricity via water electrolysis has been presented. All the examined plant configurations are based on technologies that are either commercially available or at the very least successfully demonstrated at pre-commercial scale. When the production of synthetic biofuels is maximally enhanced by an external hydrogen source (used to hydrogenate also the gasification-derived $CO_2$ to synfuels), the following increases in fuel output can be observed:

- 2.2-fold (methane) or 1.9-fold (gasoline) for designs featuring steam gasification;

[13]break-even oil price calculation based on 6 GJ/barrel, 10 $/bbl refining margin and 1.0 €/$ exchange rate.

[14]These prices are expected to represent low, medium and high prices for a wide variety of feedstock categories in Europe [35].

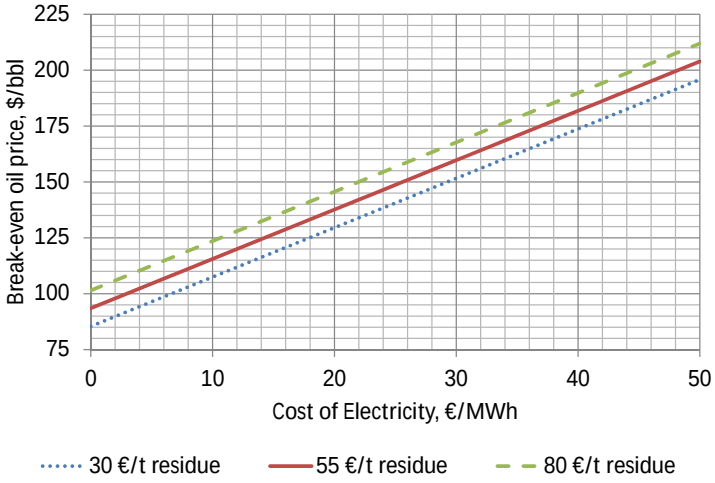


Figure 9: break-even crude oil price for OG+ plant configuration for three different biomass feedstock cost as a function of electricity price.

- 3.1-fold (methane) or 2.6-fold (gasoline) for designs featuring oxygen gasification.

Thus the increase in output is larger for plant configurations featuring oxygen gasification than steam gasification and larger for methane than gasoline production. In similar manner, the following overall carbon conversions can be achieved with enhanced configurations:

- 67.0 % (methane) and 58.4 % (gasoline) for designs featuring steam gasification;
- 98.0 % (methane) and 79.4 % (gasoline) for designs featuring oxygen gasification.

Differences in the increase of fuel output and carbon conversion arise from the higher $CO_2$ content of syngas generated via oxygen gasification,[15] higher hydrogen/carbon mole ratio of methane over synthetic gasoline, and the absence of purge gas stream in methanation in comparison to two purge gases ("carbon leaks") for the MTG route. Thus at maximum, almost all (98 % of OM+ plant) biomass carbon could be converted to saleable end-product with the presented design.

Based on the cost analysis, the conversion of gasification-derived $CO_2$ to fuels with external hydrogen becomes economically feasible when low-carbon hydrogen can be acquired at a cost that is lower than:

- 2.2 €/kg (methane) and 2.7 €/kg (gasoline) for enhanced designs featuring steam gasification;

[15] In steam gasification, a significant amount of biomass carbon is "lost" to the oxidiser's flue gas.

- 2.4 €/kg (methane) and 2.8 €/kg (gasoline) for enhanced designs featuring oxygen gasification.

To assess the relevance of these results at a wider context, the impact of hydrogen enhancement to the total supply potential[16] of synthetic biofuels in Europe has been presented in Table 7. Based on the results, 52 (gasoline) or 78 (methane) million tonnes more of oil equivalent renewable fuels could be produced in the EU area in 2030, if biorefineries were maximally enhanced with external supply of low-carbon hydrogen. This enhanced biofuel potential would amount to 41 % or 63 % of the entire transport fuel demand in 2030, respectively (see Table 7 for details). However, it can be considered unlikely that the maximum potential could ever be achieved in an economically feasible way due to the highly dispersed nature of some biomass residues. However, even when restricted only to using forestry residues (40 Mt/a, see Table 1), the hydrogen enhancement would still allow to supply 18 - 28 Mtoe/a of renewable synfuels, displacing 8 - 13 % of road transport fuel demand in 2030 annually.

Table 7: Potential biofuels output in the EU by 2030 for selected plant configurations based on 197 Mt/a residue availability. Total energy demand of 221 Mtoe for road transport is assumed in EU 2030 [36].

| Configuration | | OG | OG+ | OM | OM+ |
|---|---|---|---|---|---|
| Residue availability, 15 wt% | Mt/a | 197 | 197 | 197 | 197 |
| Residue availability, 0 wt% | Mt/a | 167 | 167 | 167 | 167 |
| Primary energy supply, 15 wt% | TWh/a | 765 | 765 | 765 | 765 |
| $H_2$ requirement | TWh/a | | 778 | | 1152 |
| Electricity requirement | TWh/a | | 1161 | | 1720 |
| Biofuel output | Mt/a | 33 | 85 | 38 | 116 |
| | Mtoe/a | 35 | 91 | 45 | 138 |
| | Mbbl/d | 0.7 | 1.8 | 0.9 | 2.8 |
| *Share of 2030 demand* | | 16 % | 41 % | 20 % | 63 % |

At the European level, maximal hydrogen enhancement of the total feedstock potential would create an additional demand for 778 - 1152 TWh/a of hydrogen or 1162 - 1720 TWh/a of low-carbon electricity if hydrogen is to be produced via water electrolysis using 67 % (LHV) efficient alkaline electrolysers.

In order to enable the reader to reproduce the performance and cost analysis presented in this paper, additional information is available in the appendices and in the online supplementry information: "Online supplementary material for Hydrogen enhancement potential of synthetic biofuels manufacture in the European context: A techno-economic assessment". The performance and cost estimates presented in this study should be taken with a measure of caution, as they are based on simulation exercises rather than collection of data from actual commercial biorefineries. As data gradually becomes available from operating facilities, actual achieved performance and costs should be considered.

[16] Food and garden waste is subtracted from total availability due to its poor suitability for thermal conversion. The data in [6] is given at 15 wt% for which 14 GJ/t LHV is assumed.

## 6. Acknowledgements

This work was carried out in the Carbon Capture and Storage Program (CCSP) research program coordinated by CLIC Innovation Oy with funding and support from Fortum Oyj, Neste Oyj, Gasum Oy, and the Finnish Funding Agency for Technology and Innovation, Tekes.

## Appendix A. Process layouts

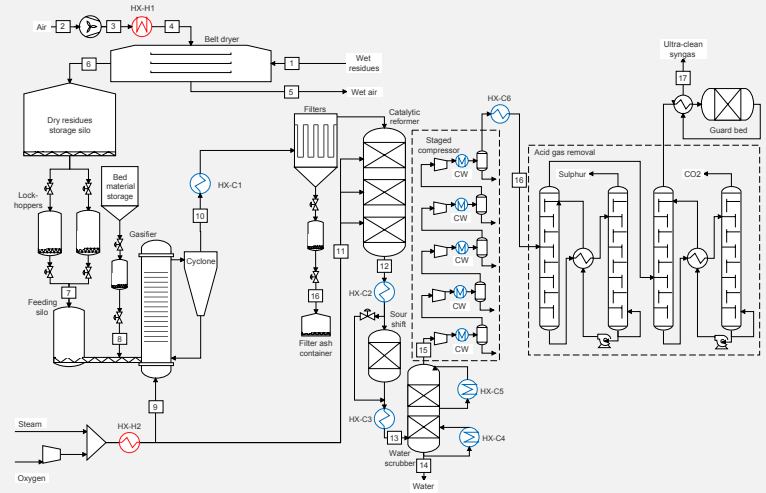


Figure A.10: Layout of synthesis gas plant based on oxygen gasification. Oxygen is produced for gasification and reforming with a cryogenic air separation unit (not shown), syngas modulus is adjusted with a sour shift reactor and syngas $CO_2$ is separated and vented by the acid gas removal unit.

## Appendix B. Additional results

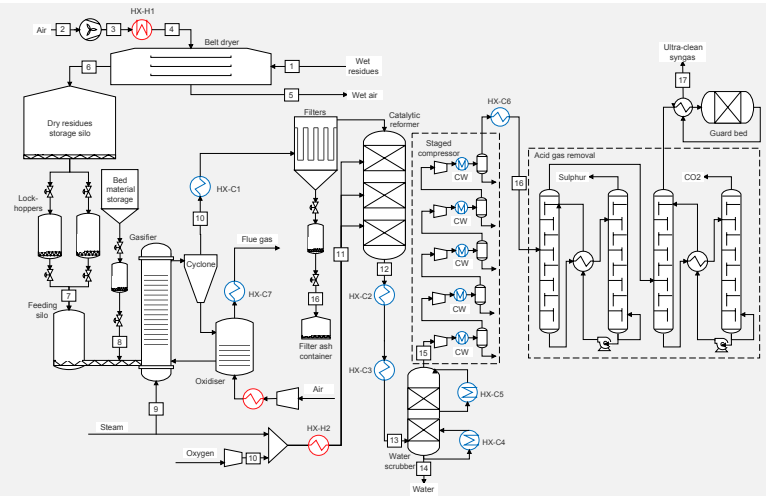


Figure A.11: Layout of synthesis gas plant based on steam gasification. Oxygen is produced for reforming with a cryogenic air separation unit (not shown), syngas modulus is adjusted with steam feed to the gasifier and syngas $CO_2$ is separated and vented by the acid gas removal unit.

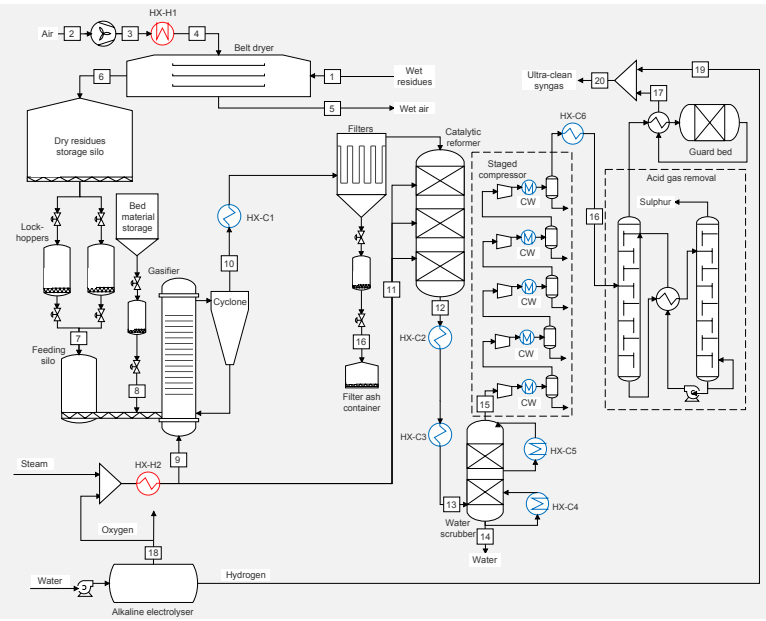


Figure A.12: Layout of synthesis gas plant based on oxygen gasification and hydrogen enhancement. Byproduct oxygen from the electrolyser is utilised for gasification and reforming and the surplus is vented to atmosphere, syngas modulus is adjusted with a correct amount of external hydrogen supply and syngas $CO_2$ is not separated.

Table B.8: Main simulation parameters for the examined plant configurations.

| **Configuration** | | OG | OG+ | OM | OM+ | SG | SG+ | SM | SM+ |
|---|---|---|---|---|---|---|---|---|---|
| **Band conveyor dryer** | | | | | | | | | |
| Specific heat consumption | $kWh/t_{evap}$ | 1300 | 1300 | 1300 | 1300 | 1300 | 1300 | 1300 | 1300 |
| Low temp. heat use | % | 20 | 20 | 20 | 20 | 20 | 20 | 20 | 20 |
| Moisture in/out | wt% | 50/15 | 50/15 | 50/15 | 50/15 | 50/15 | 50/15 | 50/15 | 50/15 |
| **Steam/$O_2$ gasifier** | | | | | | | | | |
| Pressure | bar | 4 | 4 | 4 | 4 | | | | |
| Temperature | °C | 850 | 850 | 850 | 850 | | | | |
| Heat loss (HHV) | % | 0.9 | 0.8 | 0.8 | 0.8 | | | | |
| Steam/$O_2$ | kg/kg | 1.0 | 1.0 | 1.0 | 1.0 | | | | |
| Carbon conversion | % | 98.0 | 98.0 | 98.0 | 98.0 | | | | |
| Steam/$O_2$ mix inlet temp. | °C | 215 | 215 | 203 | 203 | | | | |
| $CaCO_3$/Biomass (dry) | wt% | 2.0 % | 2.0 % | 2.0 % | 2.0 % | | | | |
| **Indirect gasifier** | | | | | | | | | |
| Pressure | bar | | | | | 2.0 | 2.0 | 2.0 | 2.0 |
| Gasification temperature | °C | | | | | 810 | 810 | 810 | 810 |
| Combustion temperature | °C | | | | | 870 | 870 | 870 | 870 |
| Heat loss | % | | | | | 1.1 | 1.1 | 1.1 | 1.1 |
| Steam/fuel (dry) | kg/kg | | | | | 0.70 | 0.80 | 0.80 | 0.80 |
| $CO_2$/fuel (dry) | kg/kg | | | | | 0.10 | 0.00 | 0.00 | 0.00 |
| Char to oxidiser/fuel(dry) | kg/kg | | | | | 0.17 | 0.16 | 0.19 | 0.19 |
| Combustion air temp. | °C | | | | | 350 | 350 | 350 | 350 |
| Steam temperature | °C | | | | | 255 | 255 | 188 | 188 |
| Fluegas end temperature | °C | | | | | 150 | 150 | 150 | 150 |
| **Filter cooler** | | | | | | | | | |
| Temp. at filter inlet | °C | 550 | 550 | 550 | 550 | 550 | 550 | 550 | 550 |
| **Reformer** | | | | | | | | | |
| Outlet temperature | °C | 950 | 950 | 850 | 850 | 950 | 950 | 850 | 850 |
| Heat loss (HHV) | % | 1.0 | 1.0 | 1.0 | 1.0 | 1.0 | 1.0 | 1.0 | 1.0 |
| Steam/$O_2$ | kg/kg | 1.0 | 1.0 | 1.0 | 1.0 | 1.0 | 1.0 | 1.0 | 1.0 |
| Methane conversion | % | 95 | 95 | 35 | 35 | 95 | 95 | 35 | 35 |
| Steam/$O_2$ mix inlet temp. | °C | 218 | 218 | 206 | 206 | 217 | 217 | 204 | 204 |
| **Sour shift** | | | | | | | | | |
| Steam/CO at inlet | mol/mol | 2.0 | | 2.0 | | | | | |
| Reactor inlet temp. | °C | 257 | | 279 | | | | | |
| Reactor outlet temp. | °C | 403 | | 404 | | | | | |
| $H_2$/CO after shift | - | 2.02 | | 3.00 | | | | | |
| **Water scrubber** | | | | | | | | | |
| Inlet temperature | °C | 200 | 200 | 200 | 200 | 200 | 200 | 200 | 200 |
| Temp. at stage 1 outlet | °C | 60 | 60 | 60 | 60 | 60 | 60 | 60 | 60 |
| Temp. at stage 2 outlet | °C | 30 | 30 | 30 | 30 | 30 | 30 | 30 | 30 |
| **Syngas compressor** | | | | | | | | | |
| Syngas pressure at outlet | bar | 21.0 | 21.0 | 16.0 | 16.0 | 21.0 | 21.0 | 16.0 | 16.0 |
| **Acid gas removal** | | | | | | | | | |
| $CO_2$ removal extent | % | 98 | 0 | 98 | 0 | 97 | 0 | 97 | 0 |
| Sulphur removal extent | % | 100 | 100 | 100 | 100 | 100 | 100 | 100 | 100 |
| **Alkaline electrolyser** | | | | | | | | | |
| Pressure | bar | | 20 | | 20 | | 20 | | 20 |
| System $H_2$ efficiency | % | | 67 | | 67 | | 67 | | 67 |
| **Low-pressure methanol** | | | | | | | | | |
| Inlet pressure | bar | 78.4 | 78.4 | | | 78.4 | 78.4 | | |
| Reactor temperature | °C | 260 | 260 | | | 260 | 260 | | |
| Extent of syngas conversion | % | 95.0 | 95.0 | | | 95.0 | 95.0 | | |
| **Methanol to gasoline** | | | | | | | | | |
| Inlet pressure | Mpa | 2.3 | 2.3 | | | 2.3 | 2.3 | | |
| DME reactor inlet temp. | °C | 297 | 297 | | | 297 | 297 | | |
| DME reactor outlet temp. | °C | 407 | 407 | | | 407 | 407 | | |
| Total MeOH conversion | % | 100 | 100 | | | 100 | 100 | | |
| **High temp. methanation** | | | | | | | | | |
| Inlet pressure | bar | | | 14.6 | 14.6 | | | 14.6 | 14.6 |
| $1^{st}$ reactor outlet temp. | °C | | | 700 | 701 | | | 701 | 700 |
| Extent of syngas conversion | % | | | 99.8 | 99.4 | | | 99.8 | 99.3 |
| **Auxiliary boiler** | | | | | | | | | |
| Boiler fluegas oxygen | mol% | 4.1 | 4.0 | 4.8 | 4.8 | | | | |
| Adiabatic flame temp. | °C | 1812 | 1811 | 1663 | 1664 | | | | |
| Fluegas to stack | °C | 150 | 150 | 150 | 150 | | | | |

Table B.9: Simulated mass and energy balances for the examined plant configurations. Electricity consumed by the electrolyser is reported as feedstock input. Mass flow of (dry) biomass into the process is 5.92 kg/s for all examined configurations.

| **Configuration** | | OG | OG+ | OM | OM+ | SG | SG+ | SM | SM+ |
|---|---|---|---|---|---|---|---|---|---|
| **Electricity balance** | | | | | | | | | |
| *On-site consumption, MW* | *MW* | *-12.5* | *-17.2* | *-9.5* | *-8.0* | *-11.4* | *-14.6* | *-7.7* | *-7.1* |
| Oxygen production | MW | -3.5 | -3.5 | -3.1 | -3.1 | -1.4 | -1.4 | -0.9 | -0.9 |
| Oxygen compression | MW | -0.7 | -0.7 | -0.6 | -0.6 | -0.1 | -0.1 | -0.1 | -0.1 |
| Feedstock pressurisation | MW | -0.2 | -0.2 | -0.2 | -0.2 | -0.1 | -0.1 | -0.1 | -0.1 |
| Feed drying | MW | -0.7 | -0.7 | -0.7 | -0.7 | -0.7 | -0.7 | -0.7 | -0.7 |
| Syngas compression | MW | -5.2 | -7.7 | -3.1 | -2.5 | -5.5 | -7.3 | -3.0 | -3.0 |
| Acid gas removal | MW | -0.9 | 0.0 | -1.0 | 0.0 | -0.7 | 0.0 | -0.7 | 0.0 |
| Synthesis | MW | -0.5 | -3.3 | -0.2 | -0.4 | -0.4 | -2.2 | -0.1 | -0.2 |
| Blowers and pumps | MW | -0.3 | -0.3 | -0.2 | -0.2 | -1.9 | -2.0 | -1.8 | -1.8 |
| Miscellaneous | MW | -0.6 | -0.8 | -0.5 | -0.4 | -0.5 | -0.7 | -0.4 | -0.3 |
| *Gross production (steam turb.)* | *MW* | *8.4* | *9.6* | *8.7* | *15.4* | *9.0* | *9.6* | *10.0* | *13.6* |
| **Steam balance** | | | | | | | | | |
| *On-site consumption* | *kg/s* | *7.9* | *6.7* | *7.2* | *5.8* | *10.5* | *10.5* | *10.0* | *9.4* |
| Gasifier | kg/s | 2.3 | 2.3 | 2.4 | 2.4 | 5.3 | 5.9 | 5.9 | 5.9 |
| Reformer | kg/s | 1.4 | 1.4 | 0.9 | 0.9 | 1.5 | 1.5 | 0.9 | 0.9 |
| AGR solvent regeneration | kg/s | 1.1 | 0.0 | 1.2 | 0.0 | 0.7 | 0.0 | 0.7 | 0.0 |
| Deaerator | kg/s | 1.4 | 1.3 | 1.2 | 1.1 | 1.3 | 1.4 | 1.1 | 1.1 |
| Economiser | kg/s | 1.7 | 1.6 | 1.5 | 1.4 | 1.6 | 1.7 | 1.4 | 1.4 |
| *Gross production* | *kg/s* | *16.4* | *21.5* | *13.8* | *22.2* | *16.8* | *19.3* | *15.0* | *19.7* |
| Syngas cooling (9.35MPa/500°C) | kg/s | 10.5 | 10.1 | 9.3 | 8.6 | 10.1 | 10.4 | 8.6 | 8.6 |
| Aux. boiler (9.35MPa/500°C) | kg/s | 2.1 | 3.7 | 0.6 | 0.6 | 3.2 | 3.4 | 3.0 | 3.0 |
| Methanation (9.35MPa/500°C) | kg/s | 0.0 | 0.0 | 4.0 | 12.9 | 0.0 | 0.0 | 3.4 | 8.0 |
| MeOH synth. (4.3MPa/255 °C) | kg/s | 3.9 | 7.7 | 0.0 | 0.0 | 3.6 | 5.5 | 0.0 | 0.0 |
| **Carbon balance** | | | | | | | | | |
| *Inputs* | | | | | | | | | |
| Biomass carbon to process | kmol/s | 0.262 | 0.262 | 0.262 | 0.262 | 0.262 | 0.262 | 0.262 | 0.262 |
| $CO_2$ feed to gasifier | kmol/s | | | | | 0.014 | | | |
| *Outputs* | | | | | | | | | |
| Carbon removed in AGR | kmol/s | 0.155 | | 0.172 | | 0.101 | | 0.093 | |
| Carbon combusted (solid) | kmol/s | 0.005 | 0.005 | 0.005 | 0.005 | 0.077 | 0.073 | 0.086 | 0.086 |
| Carbon combusted (MeOH purge) | kmol/s | 0.009 | 0.015 | | | 0.006 | 0.012 | | |
| Carbon in methane | kmol/s | | | 0.085 | 0.257 | | | 0.082 | 0.176 |
| Carbon in MTG gasoline | kmol/s | 0.080 | 0.208 | | | 0.080 | 0.153 | | |
| Carbon in MTG LPG | kmol/s | 0.009 | 0.023 | | | 0.009 | 0.017 | | |
| Carbon in MTG purge | kmol/s | 0.004 | 0.011 | | | 0.004 | 0.008 | | |
| **Oxygen balance** | | | | | | | | | |
| *On-site consumption* | kg/s | *3.7* | *3.7* | *3.2* | *3.2* | *1.5* | *1.5* | *0.9* | *0.9* |
| Gasifier | kg/s | 2.3 | 2.3 | 2.3 | 2.3 | 0.0 | 0.0 | 0.0 | 0.0 |
| Reformer | kg/s | 1.4 | 1.4 | 0.9 | 0.9 | 1.5 | 1.5 | 0.9 | 0.9 |
| *Gross production* | *kg/s* | *3.7* | *7.5* | *3.2* | *11.1* | *1.5* | *4.2* | *0.9* | *6.1* |
| $O_2$ output (ASU) | kg/s | 3.7 | | 3.2 | | 1.5 | | 0.9 | |
| $O_2$ output (AEC) | kg/s | | 7.5 | | 11.2 | | 4.2 | | 6.1 |
| **Overall energy balance** | | | | | | | | | |
| *Feedstock inputs* | | | | | | | | | |
| Biomass to dryer (50 wt-%) | MW (LHV) | 100.0 | 100.0 | 100.0 | 100.0 | 100.0 | 100.0 | 100.0 | 100.0 |
| Biomass to gasifier (15 wt-%) | MW (LHV) | 111.9 | 111.9 | 111.9 | 111.9 | 111.9 | 111.9 | 111.9 | 111.9 |
| Electricity for $H_2$ production | $MW_e$ | | 169.9 | | 251.6 | | 94.7 | | 138.5 |
| *Product outputs* | | | | | | | | | |
| Methane | MW (LHV) | | | 66.8 | 205.4 | | | 63.7 | 139.9 |
| Gasoline | MW (LHV) | 51.8 | 134.0 | | | 51.0 | 98.0 | | |
| LPG | MW (LHV) | 6.1 | 15.8 | | | 6.0 | 11.5 | | |
| MTG purge | MW (LHV) | 3.0 | 7.8 | | | 3.0 | 5.7 | | |
| Net electricity to grid | $MW_e$ | -4.1 | -177.5 | -0.8 | -244.2 | -2.4 | -99.6 | 2.3 | -131.9 |
| District heat (steam cycle) | $MW_{th}$ | 13.0 | 19.9 | 5.9 | 30.3 | 14.8 | 21.5 | 11.2 | 23.4 |
| District heat (MeOH synth.) | $MW_{th}$ | | 9.8 | | | | | | |
| District heat (methanation) | $MW_{th}$ | | | 2.8 | 16.4 | | | 2.4 | 11.0 |
| Low temperature heat | $MW_{th}$ | 2.2 | 2.0 | 2.1 | 1.9 | 3.1 | 3.2 | 2.8 | 2.8 |

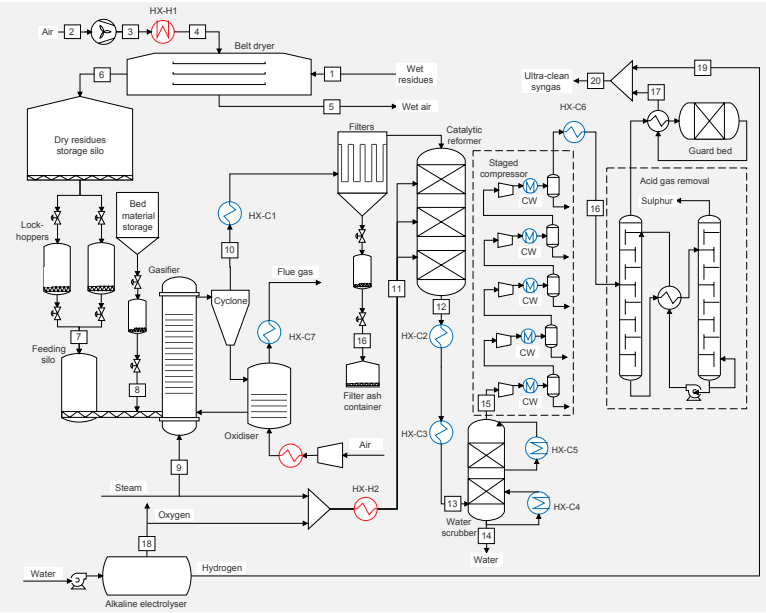


Figure A.13: Layout of synthesis gas plant based on steam gasification and hydrogen enhancement. Byproduct oxygen from the electrolyser is utilised for reforming and the surplus is vented to atmosphere, syngas modulus is adjusted with a correct amount of external hydrogen supply and syngas $CO_2$ is not separated.

Table B.10: Total capital investment estimates for the examined plant configurations based on 100 MW (LHV) biomass input, excluding equipment needed for external hydrogen generation. Part of the steam gasifier investment is reported in the row 'HRSG, oxidiser and steam cycle'

| **Configuration** | **OG** | **OG+** | **OM** | **OM+** | **SG** | **SG+** | **SM** | **SM+** |
|---|---|---|---|---|---|---|---|---|
| **Installed equipment cost** | | | | | | | | |
| Civil works | 5 | 5 | 5 | 5 | 5 | 5 | 5 | 5 |
| Cryogenic ASU | 15 | | 14 | | 10 | | 8 | |
| Feedstock pretreatment | 9 | 9 | 9 | 9 | 9 | 9 | 9 | 9 |
| Gasification | 17 | 17 | 17 | 17 | 8 | 8 | 8 | 8 |
| Hot-gas cleaning | 14 | 14 | 13 | 13 | 14 | 15 | 14 | 14 |
| CO shift | 2 | | 2 | | | | | |
| Scrubber | 3 | 3 | 3 | 3 | 3 | 3 | 3 | 3 |
| Syngas compression | 3 | 3 | 3 | 3 | 3 | 3 | 2 | 2 |
| Acid gas removal | 20 | 10 | 20 | 10 | 18 | 10 | 16 | 9 |
| HRSG, oxidiser and steam cycle | 20 | 22 | 20 | 27 | 35 | 35 | 37 | 41 |
| Additional syngas compression | 2 | 3 | | | 2 | 3 | | |
| Guard beds and methanol loop | 17 | 37 | | | 17 | 30 | | |
| Distillation (minimal) | 2 | 5 | | | 2 | 4 | | |
| MTG synthesis | 27 | 51 | | | 27 | 42 | | |
| Guard beds and methanation | | | 18 | 44 | | | 16 | 33 |
| **Sum of installed equipment cost** | **156** | **179** | **123** | **131** | **153** | **167** | **119** | **125** |
| Indirect costs | 20 | 23 | 15 | 16 | 19 | 21 | 14 | 15 |
| Contingency | 32 | 38 | 22 | 21 | 29 | 33 | 20 | 19 |
| Unscheduled equipment | 16 | 18 | 12 | 13 | 15 | 17 | 12 | 12 |
| **Total plant cost** | **223** | **259** | **173** | **181** | **216** | **238** | **165** | **171** |
| Interest during construction | 11 | 13 | 9 | 9 | 11 | 12 | 8 | 8 |
| **Total capital investment** | **234** | **272** | **182** | **190** | **227** | **250** | **173** | **180** |

[1] C. Le Quéré, R. J. Andres, T. Boden, T. Conway, R. A. Houghton, J. I. House, G. Marland, G. P. Peters, G. R. van der Werf, A. Ahlström, R. M. Andrew, L. Bopp, J. G. Canadell, P. Ciais, S. C. Doney, C. Enright, P. Friedlingstein, C. Huntingford, A. K. Jain, C. Jourdain, E. Kato, R. F. Keeling, K. Klein Goldewijk, S. Levis, P. Levy, M. Lomas, B. Poulter, M. R. Raupach, J. Schwinger, S. Sitch, B. D. Stocker, N. Viovy, S. Zaehle, N. Zeng, The global carbon budget 1959-2011, Earth System Science Data 5 (1) (2013) 165–185. doi:10.5194/essd-5-165-2013.

[2] D. Hartmann, A. K. Tank, M. Rusticucci, L. Alexander, S. Brnnimann, Y. Charabi, F. Dentener, E. Dlugokencky, D. Easterling, A. Kaplan, B. Soden, P. Thorne, M. Wild, P. Zhai, Observations: Atmosphere and surface, in: T. Stocker, D. Qin, G.-K. Plattner, M. Tignor, S. Allen, J. Boschung, A. Nauels, Y. Xia, V. Bex, P. Midgley (Eds.), Climate Change 2013: The Physical Science Basis. Contribution of Working Group I to the Fifth Assessment Report of the Intergovernmental Panel on Climate Change, Cambridge University Press, Cambridge, United Kingdom and New York, NY, USA, 2013.

[3] IPCC, Climate Change 2007: Synthesis Report. Contribution of Working Groups I, II and III to the Fourth Assessment Report of the Intergovernmental Panel on Climate Change, IPCC, Geneva, Switzerland, 2007, p. 104.

[4] IPCC, Summary for policymakers, in: O. Edenhofer, R. Pichs-Madruga, Y. Sokona, E. Farahani, S. Kadner, K. Seyboth, A. Adler, I. Baum, S. Brunner, P. Eickemeier, B. Kriemann, J. Savolainen, S. Schlmer, C. von Stechow, T. Zwickel, J. Minx (Eds.), Climate Change 2014: Mitigation of Climate Change. Contribution of Working Group III to the Fifth Assessment Report of the Intergovernmental Panel on Climate Change, Cambridge University Press, Cambridge, United Kingdom and New York, NY, USA, 2014.

[5] IEA, Technology Roadmap - Biofuels for Transport, International Energy Agency (2011). URL http://bit.ly/1MqB4Kd

[6] S. Searle, C. Malins, Availability of cellulosic residues and wastes in the EU, White paper, The International Council on Clean Transportation (2013).

[7] EU transport in figures: Statistical pocketbook 2014, European Union, Luxembourg: Publications Office of the European Union, 2014.

[8] I. Landälv, Demonstration plants for advanced biofuels production based on thermochemical pathways - status and reflections, in: Proceedings of the 21st European Biomass Conference and Exhibition, Copenhagen, Denmark, 2013.

[9] Neste Oil, Stora Enso shelve plans for renewable diesel plant, Biomass magazine, August 22, 2012. URL http://bit.ly/1mUBfPz

[10] Report from the bio-DME plant in Piteå, ChemrecNews, May, 2012. URL http://bit.ly/1u9aIlN

[11] Haldor Topsøe and partners produce biobased gasoline, Biomass magazine, June 26, 2013. URL http://bit.ly/1mUBv0U

[12] M. Hedenskog, Gasification of forest residues - IRL in a large demonstration scale, Presentation at IEA biomass gasification workshop in Karlsruhe, Göteborg Energi (2014). URL http://bit.ly/1OmgA4p

[13] D. Mignard, C. Pritchard, On the use of electrolytic hydrogen from variable renewable energies for the enhanced conversion of biomass to fuels, Chemical Engineering Research and Design 86 (5) (2008) 473 – 487. doi:10.1016/j.cherd.2007.12.008.

[14] J. B. Hansen, I. Dybkjaer, C. F. Pedersen, J. U. Nielsen, N. Christiansen, SOEC enabled methanol synthesis, in: 10th European SOFC Forum 2012, Lucerne, Switzerland, 2012.

[15] M. Pozzo, A. Lanzini, M. Santarelli, Enhanced biomass-to-liquid BTL conversion process through high temperature co-electrolysis in a solid oxide electrolysis cell SOEC, Fuel 145 (2015) 39 – 49. doi:10.1016/j.fuel.2014.12.066.

[16] I. Hannula, Co-production of synthetic fuels and district heat from biomass residues, carbon dioxide and electricity: Performance and cost analysis, Biomass and Bioenergy 74 (2015) 26 – 46. doi:10.1016/j.biombioe.2015.01.006.

[17] C. Wilen, A. Moilanen, E. Kurkela, Biomass feedstock analyses, VTT Publications 282, Technical Research Centre of Finland, VTT (1996).

[18] E. Kurkela, M. Kurkela, I. Hiltunen, The effects of wood particle size and different process variables on the performance of steam-oxygen blown circulating fluidized-bed gasifier, Environmental Progress & Sustainable Energy 33 (3) (2014) 681–687. doi:10.1002/ep.12003.

[19] P. Simell, I. Hannula, S. Tuomi, M. Nieminen, E. Kurkela, I. Hiltunen, N. Kaisalo, J. Kihlman, Clean syngas from biomass - Process development and concept assessment, Biomass Conversion and Biorefinery (2014) 1–14doi:10.1007/s13399-014-0121-y.

[20] N. Kaisalo, J. Kihlman, I. Hannula, P. Simell, Reforming solutions for biomass-derived gasification gas experimental results and concept assessment, Fuel 147 (2015) 208 – 220. doi:10.1016/j.fuel.2015.01.056.

[21] E. Kurkela, P. Simell, P. McKeough, M. Kurkela, Production of synthesis gas and clean fuel gas [Synteesikaasun ja puhtaan polttokaasun valmistus], VTT Publications 682, Technical Research Centre of Finland, VTT (2008).

[22] I. Hannula, E. Kurkela, A parametric modelling study for pressurised steam/$O_2$-blown fluidised-bed gasification of wood with catalytic reforming, Biomass and Bioenergy 38 (2012) 58–67, Overcoming Barriers to Bioenergy: Outcomes of the Bioenergy Network of Excellence 2003-2009. doi:10.1016/j.biombioe.2011.02.045.

[23] I. Hannula, E. Kurkela, Liquid transportation fuels via large-scale fluidised-bed gasification of lignocellulosic biomass, VTT Technology 91, Technical Research Centre of Finland (2013).

[24] J. Ivy, Summary of electrolytic hydrogen production - Milestone completion report, Tech. Rep. NREL/MP-560-36734, National Renewable Energy Laboratory (2004).

[25] P. Sabatier, J. Senderens, Nouvelles syntheses du methane, Acad Sci 314 (1902) 514–6.

[26] P. Tijm, F. Waller, D. Brown, Methanol technology developments for the new millennium, Applied Catalysis A: General 221 (1-2) (2001) 275–282, Hoelderich Special Issue. doi:10.1016/S0926-860X(01)00805-5.

[27] M. Patart, French patent 540 343 (1921).

[28] Converter options for methanol synthesis, Nitrogen 210 (1994) 36–44.

[29] E. Jorn, J. Rostrup-Nielsen, Process for the preparation of hydrocarbons, Patent US 4481305, Haldor Topsøe A/S (1984).

[30] Wiley Critical Content - Petroleum Technology, Vol.1-2, John Wiley & Sons, 2007.

[31] J. Penick, W. Lee, J. Maziuk, Development of the methanol-to-gasoline process, in: Chemical Reaction Engineering - Plenary Lectures, ACS Symposium Series, Vol. 226, 1983, Ch. 3, pp. 19–48.

[32] S. Yurchak, Development of Mobil's fixed-bed methanol-to-gasoline (MTG) process, Stud.Surf.Sci.Catal. 36 (1988) 251–272.

[33] J. Black, Cost and performance baseline for fossil energy plants volume 1: Bituminous coal and natural gas to electricity, Revision 2a, September 2013 DOE/NETL-2010/1397, U.S. National Energy Technology Laboratory (2007).

[34] G. Liu, E. D. Larson, R. H. Williams, T. G. Kreutz, X. Guo, Supporting information for making Fischer-Tropsch fuels and electricity from coal and biomass: Performance and cost analysis, Energy & Fuels 25 (1). doi:10.1021/ef101184e.

[35] D. Turley, G. Evans, L. Nattrass, Use of sustainably-sourced residue and waste streams for advanced biofuel production in the european union: rural economic impacts and potential for job creation, A report for the european climate foundation, NNFCC (2013).

[36] E4tech, EU 2030 Road Transport Decarbonisation Scenario Analysis (2014). [link].
URL bit.ly/1OtunVN

Online supplementary material for

# Hydrogen enhancement potential of synthetic biofuels manufacture in the European context: A techno-economic assessment

Ilkka Hannula
VTT Technical Research Centre of Finland Ltd.

April 16, 2016

## Contents

# Appendix A: Process design parameters for ASPEN Plus® simulations

Process design parameters for ASPEN Plus® simulations are given in the table below.

Table 1: Summary of process design parameters.

| Item | Design parameters | Notes |
|---|---|---|
| Air separation unit | Oxygen delivered from ASU at 1.05 bar pressure. Oxygen product (mol-%): $O_2$ = 99.5 %, $N_2$ = 0.5 %, Ar = 0 %. Power consumption 263kWh/ton$O_2$. | a |
| Feedstock preparation and handling | Feeding screw power consumption 7 kJ/kg biomass. Lock-hopper inert gas consumption: 0.07642 $Nm^3$/kg biomass for a double lock-hopper system that uses purge gas from LH to partly pressurise another LH. For a single lock-hopper system inert gas consumption 50 % higher. | b |
| Atmospheric band conveyor dryer | Biomass moisture: inlet 50 wt-%, outlet 15 wt-%, hot water: $T_{in}$=90 °C, $T_{out}$=60 °C, steam: 0.8 bar & 94 °C, heat consumption: 1300kWh/ton$H_2O_{evap}$, power consumption: 32 kWh/$ton_{drybio}$ | c |
| Pressurised circulating fluidised-bed steam/$O_2$ gasifier | Heat loss = 1 % of biomass LHV. Δp = -0.2 bar. Carbon conversion: 98 %. Modelled in two steps with RStoic and RGibbs using Redlich-Kwong-Soave equation of state with Boston-Mathias modification (RKS-BM). Hydrocarbon formation (kmol/kg of fuel volatiles): $CH_4$ = 6.7826, $C_2H_4$ = 0.4743, $C_2H_6$ = 0.2265, $C_6H_6$ = 0.2764. Tars modelled as naphthalene: $C_{10}H_8$ = 0.0671, All fuel nitrogen converted to $NH_3$. All other components assumed to be in simultaneous phase and chemical equilibrium. | d, e |
| Atmospheric circulating fluidised-bed steam gasifier | Heat loss = 1 % of biomass LHV. Δp = -0.2 bar. Modelled with RStoic and RGibbs using Redlich-Kwong-Soave equation of state with Boston-Mathias modification (RKS-BM). Hydrocarbon formation (kmol/kg of fuel volatiles): $CH_4$ = 9.0, $C_2H_4$ = 0.727, $C_2H_6$ = 0.2378, $C_6H_6$ = 0.1787. Tars modelled as naphthalene: $C_{10}H_8$ = 0.0261, All fuel nitrogen converted to $NH_3$. All other components assumed to be in simultaneous phase and chemical equilibrium. | d, e |
| Ceramic hot-gas filter | Δp = -0.2 bar. Inlet temperature 550°C. | e |
| Catalytic autothermal partial oxidation reformer | Modelled as RGibbs using Redlich-Kwong-Soave equation of state with Boston-Mathias modification (RKS-BM). Phase and chemical equilibrium conversion for $C_{2+}$ and tar. Ammonia conversion restricted to 50%. Outlet temperature and $CH_4$ conversion: 957 °C & 95 % or 850 °C & 35 % depending on the case investigated. Δp = -0.2 bar | d, e |
| Sour shift | $T_{out}$ = 404°C, steam/CO = 1.8 mol/mol, Δp = -0.2 bar. Modelled as REquil using Redlich-Kwong-Soave equation of state with Boston-Mathias modification (RKS-BM). Equilibrium reactions: CO + $H_2O$ = $CO_2$ + $H_2$, $T_{appr}$ = 10 K. COS + $H_2O$ = $CO_2$ + $H_2S$, $T_{appr}$ = 0 K. HCN + $H_2O$ = CO + $NH_3$, $T_{appr}$ = 10 K. | f, e |
| Scrubber | Scrubbing liquid: water. $T_{inlet}$ 200°C. Two-step cooling: $T^1_{out}$= 60°C, $T^2_{out}$= 30°C. Complete ammonia removal. Modelled as Flash using Soave-Redlich-Kwong (SRK) equation of state model. | e |
| Rectisol acid gas removal | 100 % $H_2S$ capture, for $CO_2$ capture level see case designs. Utilities: Electricity (other than for refrigeration) = 1900kJ/kmol($CO_2$+$H_2S$); Refrigeration 3 x duty needed to cause -12 K temperature change in the syngas; 5 bar steam = 6.97 kg/kmol ($H_2S$+$CO_2$). | g |

Table 1 – concluded from previous page

| Item | Design parameters | Notes |
|---|---|---|
| High temperature methanation | Six adiabatic fixed-bed reactors connected in series and equipped with intercoolers. Pressure at system inlet = 15 bar, pressure at system outlet 11 bar. $T_{input}$ to reactors 300 °C. $T_{output}$ from the first reactor restricted to 700 °C with steam dilution. Gas dried before feeding to last reactor. Syngas conversion to methane >99.5 %. Equilibrium reactions: $CO + 3H_2 = CH_4 + H_2O$, $T_{appr.}$ = 20 K; $CO_2 + 4H_2 = CH_4 + 2H_2O$, $T_{appr.}$ = 20 K. Reactors modelled as REquils using Soave-Redlich-Kwong (SRK) equation of state model. | e |
| Low-pressure methanol synthesis | $T_{reaction}$= 260°C, $P_{fresh\ feed}$= 80bar, Δp =-5bar, Boiling-water reactor modelled with REquil using Soave-Redlich-Kwong equation of state (SRK). Equilibrium reactions: $CO + 2H_2 = CH_4O$, $T_{appr.}$ = 10 K; $CO_2 + 3H_2 = CH_4O + H_2O$, $T_{appr.}$ = 10 K. | e |
| Methanol to Gasoline | DME reactor: $T_{in}$= 297°C, $T_{out}$=407°C, $P_{in}$= 23bar, Δp =-1bar, Boiling-water reactor modelled with REquil using Soave-Redlich-Kwong equation of state (SRK). Equilibrium reaction: $2CH_4O = C_2H_6O + H_2O$, $T_{appr}$ = 30 K. Gasoline reactor: $T_{reactor}$= 400°C, $P_{in}$= 22bar, Δp =-1bar, Modelled as REquil using Soave-Redlich-Kwong equation of state (SRK). Relative mass yields from 1 tonne of raw product in the refining area are 880 kg of gasoline blendstock, 100 kg of LPG and 20 kg of purge gas. | h |
| Alkaline electrolysis | $H_2$ and $O_2$ purity 100 %. Both delivered at 20 bar pressure and 25 °C, Electrolyser system efficiency = 67 % (LHV). | e, i |
| Auxiliary boiler | Modelled as RStoic, Δp = - 0.1bar, Lambda = 1.20, Air preheat to 250°C with flue gas | e |
| Heat exchangers | $\Delta p/p$ = 2 %; $\Delta T_{min}$ = 15°C (gas-liq), 30 °C (gas-gas). Heat loss = 1 % of heat transferred. | g |
| Heat recovery & Steam system | Flue gas $T_{out}$=150°C, feed water pressure 110 bar, steam drum blowdowns: 2 % of inlet flow, Deaerator $T_{out}$ = 120°C. | e |
| Steam turbine | Inlet steam parameters: 93.5 bar, 500°C; Extraction steam parameters: HP = 25 bar, 330°C; LP = 5 bar, 179°C; $\eta_{isentropic}$ = 0.78, $\eta_{generator}$=0.97 , $\eta_{mechanical}$=0.98. | c, e, j |
| Compressors | Stage pressure ratio <2, $\eta_{polytropic}$= 0.85, $\eta_{driver}$= 0.92, $\eta_{mechanical}$= 0.98. | k |
| Multistage compressors (>4.5 kg/s) | Stage pressure ratio <2, $\eta_{polytropic}$= 0.87, $\eta_{driver}$= 0.92, $\eta_{mechanical}$= 0.98, $T_{intercooler}$= 35°C, $\Delta p/p_{intercooler}$= 1 %. | l |
| Multistage compressors (<4.5 kg/s) | Stage pressure ratio <2, $\eta_{polytropic}$= 0.85, $\eta_{driver}$= 0.90, $\eta_{mechanical}$= 0.98, $T_{intercooler}$= 35°C, $\Delta p/p_{intercooler}$= 1%. | l |
| Pumps | $\eta_{hydraulic}$= 0.75, $\eta_{driver}$ = 0.90. | k |

a - Taken from Smith et al. [1].
b - Taken from Swanson et al. [2]. The original value in the reference was given for bagasse (160 kg/m$^3$), which is here fitted for forest residues (293 kg/m$^3$) assuming that LH is filled with feedstock up to 90 %.
c - Based on personal communication with Andras Horvath, Carbona-Andritz, May 15$^{th}$ 2012.
d - Modelling principles taken from Refs. [3] and [4].
e - Operating parameters chosen by the author.
f - Outlet temperature and steam/CO ratio based on personal communication with Wolfgang Kaltner, Süd-Chemie AG, July 9$^{th}$, 2012.
g - Taken from Liu et al. [5].
h - Taken from Larson et al. [6].
i - System efficiency calculation based on information taken from ETOGAS news on July 28th 2015.
j - Based on personal communication with Reijo Kallio, ÅF-Consult, October 2012.
k - Taken from Chiesa et al. [7].
l - Taken from Glassman [8].

# Appendix B: Equipment cost database & factors for Total Plant Cost estimation

Capital cost estimates were used as basis for evaluating the prospective economics of synthetic fuel production. These estimates were based on a self-consistent set of component-level capital cost data assembled using literature sources, vendor quotes and discussions with industry experts. When data for a given piece of equipment was unattainable, the costs were estimated based on similar equipment and engineering judgement. A summary of the equipment cost database used in this work is given in Table 2. All equipment costs have been escalated to correspond with 2010 euros using *Chemical Engineering* magazine's Plant Cost Index to account for inflation.

Table 2: Reference equipment costs database with cost factors employed in estimating Total Plant Costs.

| **Cost component** | **CSP** | **$S_0$** | **UEC** | **IC** | **$C_0$** | **IDC** | **PC** | **k** | **Notes** |
|---|---|---|---|---|---|---|---|---|---|
| Civil works | Feed, $MW_{th}$ | 300 | | | 12.8 | 10 % | 30 % | 0.85 | a |
| ASU incl. compr. | Oxygen, t/h | 76.6 | | | 36.8 | 10 % | 10 % | 0.50 | b |
| Feedstock handling | Feed, $MW_{th}$ | 157 | | | 5.3 | 10 % | 10 % | 0.31 | c |
| Belt dryer | Water evap, kg/s | 0.342 | | | 1.9 | 10 % | 10 % | 0.28 | d |
| Pressurised $O_2$ CFB gasifier | Dry biom, kg/s | 17.8 | 25.1 | 50 % | 37.7 | 15 % | 30 % | 0.75 | a |
| Atm. steam CFB gasifier | Dry biom, kg/s | 17.8 | 12.6 | 50 % | 18.9 | 15 % | 30 % | 0.75 | a |
| Ceramic hot-gas filter | Syngas, kmol/s | 1.466 | 5.9 | 15 % | 6.8 | 15 % | 30 % | 0.67 | a |
| Catalytic reformer | Syngas, kmol/s | 2.037 | 14.5 | 50 % | 21.8 | 15 % | 30 % | 0.67 | a |
| WGS stage | Gasif. feed, $MW_{th}$ | 1377 | | | 12.6 | 15 % | 30 % | 0.67 | e |
| Scrubber | Syngas, kmol/s | 1.446 | | | 5.2 | 15 % | 30 % | 0.67 | a |
| Syngas compr. | Compr. work, $MW_e$ | 10 | | | 5.0 | 15 % | 30 % | 0.67 | f |
| $CO_2$ compr. | Compr. work, $MW_e$ | 10 | | | 5.0 | 15 % | 30 % | 0.67 | f |
| $O_2$ compr. | Compr. work, $MW_e$ | 10 | | | 5.7 | 15 % | 30 % | 0.67 | f |
| $H_2$ compr. | Compr. work, $MW_e$ | 10 | | | 5.7 | 15 % | 30 % | 0.67 | g |
| AGR incidentals compr. | Compr. work, $MW_e$ | 10 | | | 5.0 | 15 % | 30 % | 0.67 | f |
| AGR | kNm3/hr (NTP) | 200 | 49.3 | 15 % | 56.7 | 15 % | 30 % | 0.63 | h |
| Alkaline electrol. | Power, $MW_e$ | 9 | | | 9 | 10 | 0 % | 1 | i |
| HRSG | Heat transf, $MW_{th}$ | 43.6 | 5.2 | 15 % | 6.0 | 15 % | 30 % | 0.80 | b |
| Aux. boiler & fluegas treatm. | Feed, $MW_{th}$ | 5.9 | 5.1 | 15 % | 5.9 | 10 % | 10 % | 0.65 | j, k |

Table 2 – concluded from previous page

| Cost component | CSP | $S_0$ | UEC | IC | $C_0$ | IDC | PC | k | Notes |
|---|---|---|---|---|---|---|---|---|---|
| Steam turbine unit | Power, $MW_e$ | 15.2 | 6.8 | 15 % | 7.8 | 10 % | 10 % | 0.85 | j, l |
| CHP equipment | Power, $MW_e$ | 15.2 | 4.1 | 15 % | 4.7 | 10 % | 10 % | 0.85 | j, m |
| Other steam cycle equipment | Power, $MW_e$ | 15.2 | 6.3 | 15 % | 7.3 | 10 % | 10 % | 0.85 | j, n |
| Guard beds | Syngas, $MW_{th}$ | 260 | 5.2 | 15 % | 6.0 | 10 % | 10 % | 0.85 | o |
| MeOH loop | MeOH, $MW_{th}$ | 210 | 28.3 | 15 % | 32.5 | 10 % | 10 % | 0.67 | o |
| Methanol distill. (mini-mum) | MeOH, $MW_{th}$ | 210 | 4.2 | 15 % | 4.8 | 10 % | 10 % | 0.88 | o, p |
| Methanol distill. (chem-grade) | MeOH, $MW_{th}$ | 210 | 12.6 | 15 % | 14.5 | 10 % | 10 % | 0.88 | o, p |
| Methanation equipment | Methane, $MW_{th}$ | 210 | 28.3 | 15 % | 32.5 | 15 % | 30 % | 0.67 | q |
| MTG DME reactor | Gasoline, bbl/day | 16 667 | | | 45.3 | 15 % | 30 % | 0.67 | r |
| MTG gasoline reactor | Gasoline, bbl/day | 16 667 | | | 101.2 | 15 % | 30 % | 0.67 | r |
| MTG gasoline finisher | Gasoline, bbl/day | 5 556 | | | 8.2 | 15 % | 30 % | 0.67 | r |

Note: $C_0$ is the cost of an installed reference equipment of size $S_0$ in 2010 euros and $k$ is the cost scaling factor. CSP stands for cost scaling parameter, UEC for uninstalled equipment cost, IC for installation costs, IDC for indirect costs and PC for project contingency.
a - Author's estimate.
b - Taken from Larson et al. [9].
c - Costs taken from Ref. [10]. Scaling exponent calculated from two different size handling systems using feedstock energy flow as scaling parameter.
d - Reference capacity and costs taken from Ref. [10]. Scaling exponent calculated based on information on two different size dryers using water removal rate as scaling parameter. Drying capacity is increased by extending the dryer, which results in unusually low scaling factor (middle parts are fairly affordable in comparison to the ends of the dryer).
e - Extracted from Kreutz et al. [11]. This cost is for two-stage equipment that includes balance of plant (15 %) and indirect costs (15 %). It is assumed that a single-stage adiabatic sour shift reactor is 40 % of the cost of a two-stage system (see Ref. [5]). Balance of plant and indirect costs have been removed.
f - Taken from Kreutz et al. [11].
g - It is likely that a $H_2$ compressor is more expensive than an $O_2$ compressor of similar size (electricity usage), but in the lack of reliable cost data an equal cost is assumed.
h - This cost is for a Rectisol system that separates $CO_2$ and $H_2S$ into separate streams (separate column for each compound). Taken from Liu et al. [5].
i - Based on a investment announcement mady by Woikoski Oy in Finland in 2014.
j - Costs based on Thermoflow PEACE equipment cost estimator and discussions with experts at ÅF-Consult.
k - Includes boiler and related systems such as air preheaters, fans, ducts, stack, fabric filter et cetera.
l - Includes turbine, generator and electrification related to the delivery.
m - Includes items such as a water cooled condenser, district heaters, deaerator et cetera.
n - Includes items such as tanks, pumps, fans, makeup water system, fuel & ash handling systems et cetera.
o - Taken from Ref. [12], originally based on a quotation from Haldor Topsøe in September 2003. Recalculated.
p - Cost (down) scaling factor from Wan [13].
q - Methanation system is assumed to have the same cost as a methanol loop (i.e. distillation equipment excluded) with equal fuel output.
r - Taken from Larson et al. [6]. Approximately one third of the raw gasoline from MTG reactors is processed through a finisher.

# Appendix C: Technology descriptions

The following text aims to expand and deepen the technology descriptions available in the original research paper in order to provide the reader with a fuller understanding of the technologies behind the analysis.

## Feedstock handling and drying

Feedstock pretreatment is an important part of almost every biomass conversion process. The specific arrangement of a particular pretreatment chain is dependent on the type of feedstock and conversion technology, but usually includes at least transfer, storage, chipping, crushing and drying of feedstock [14]. Operating problems with fuel feeding and handling equipment are the most common denominator for unforeseen shutdowns of biomass conversion processes and reliable solids handling systems are thus essential to successful operation of the plant [15].

### Pretreatment

Since feed preparation and handling equipment are often expensive and require heat and power to operate, it is preferable to minimise the pretreatment requirement of the conversion process. Fluidised-bed gasifiers are characterised by their wide feedstock base and their ability to convert low-quality feedstocks into synthesis gas. Only minor pretreatment requirements are thus imposed for the considered feedstock. For forest residues this means mainly chipping down to a maximum length of 50 mm, which can take place either at the harvesting site or alternatively after transportation at the conversion plant.

Forest residues typically have a moisture content of about 50 wt% and a LHV around 8 - 9 MJ/kg. In order to improve the quality of synthesis gas and to increase thermal efficiency of the overall conversion process, chips are dried down to 15 wt% (LHV 16.07 MJ/kg) by utilising low temperature by-product heat sources available from the gasification plant. Drying of biomass to a low moisture contents is problematic and has not been fully optimised for biomass conversion processes [14], although atmospheric band conveyor dryers (belt dryer) can be considered available for reliable execution.

### Belt dryer

Belt dryers operate by blowing hot drying medium through a thin layer of feedstock on a permeable belt moving horizontally through the enclosed drying chamber [16]. A belt dryer can be realised based on three different basic designs: i) a single-stage single-pass design, where a continuous single band carries the feedstock through the whole length of the dryer; ii) a multi-stage single-pass design, where a number of belts are arranged in series so that when fuel reaches the end of a belt, it falls onto the beginning of the next, exposing new feedstock surfaces to drying medium; iii) a multi-stage multi-pass design, where several belts are installed one above the other so that each will discharge its feedstock onto the belt below (see Fig. 1). The drying medium is moved through the dryer by a number of fans and can flow either in co- or counter-current with respect to the passage of feedstock [16].

According to an advertorial brochure [17], belt dryers can be used to dry biomass down to 8 wt% moisture content using various low temperature heat sources. They enable close control of residence time and temperature and due to the relatively thin layer of feedstock on the conveyer belt, a good uniformity of drying is achieved [14]. A single belt dryer is able to evaporate water up to a rate of 20 tonnes per hour and when several dryers are needed, they can be stacked on top of each other to save floor space. Plant configurations examined in this thesis feature belt dryers that operate with hot water (90 °C in, 60 °C out) produced from heat recovered from the first cooling stage of the water scrubber and/or low-pressure steam extracted from the turbine. 20% of the belt dryer's overall heat requirement is satisfied with low (< 60 °C) temperature heat.

The specific energy consumption and evaporation capacity of a dryer depends on the feedstock moisture, inlet and outlet temperature of the drying medium as well as structure and particle size of the feedstock. Based on discussions with industry experts, the specific heat consumption of a belt dryer has been set to 1300 kWh/$t_{H_2O}$ evaporated, and power consumption at 32 kWh/tonne of dry feedstock.

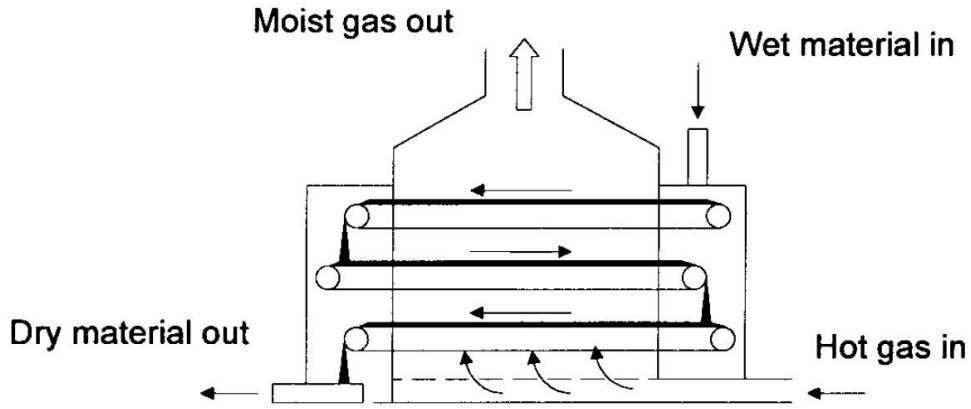


Figure 1: An operating principle of a multi-stage multi-pass belt conveyor dryer [16].

**Feeding against pressure**

The handling characteristics of biomass are affected by quality, moisture content, particle size and amount of impurities. Pressure is also known to cause changes in the tension and compression strength of the feedstock, which affects its flow characteristics and thus its behaviour in the feeding equipment [15]. A wide variety of equipment designs for feeding biomass feedstocks into pressurised reactors have been developed since the 1950s, mainly in conjunction with the development of continuous commercial-scale processes in the pulp and paper industries. Some of the designs were adapted from feeders used in pressurised combustion and gasification of coal, although several modifications were required due to biomass' low bulk density and increased resistance to flow. In general, three types of feeding equipment can be considered for feeding dry biomass into high-pressure reactors: rotary valves, lock hoppers and plug feed systems. An ideal biomass pressure feeder would be 1) highly reliable, 2) have low capital, operating and maintenance costs, 3) be suitable for wide range of feedstocks, 4) and have accurate feed control. However, all requirements cannot usually be reached with any single feeder type and compromises must be made.

The suitability of different pressure feeders for biomass applications have been assessed by Rautalin and Wilén [15] and more recently also by Lau et al. [18]. Out of the several types of feeders, the lock hopper-based system is a preferred choice for dry biomass as it has been extensively tested with various biomass feedstocks and is generally considered to be a well-proven system. Lock hopper systems have been used by Lurgi and others for feeding up to 70 tonnes/h of coal at pressures as high as 90 bars [18]. For biomass feedstocks the design has been modified to include a live bottom metering bin, equipped with a multiscrew system for metering the fuel to the injector screw of the pressurised gasifier [15]. Despite these modifications, lock hopper feeding systems offer the advantage of a simple design with few moving parts and the ability to handle a wide variety of biomass fuel types [18].

The operating principle of a lock hopper system is based on a feeding sequence that begins by feeding a batch of fuel via feed hopper into the lock hopper. A valve separating the hoppers is closed and the lock hopper is pressurised with inert gas. After pressure is equalised with a metering bin below, the bottom valve is opened, which causes fuel to flow into the bin by gravity. After the lock hopper has been vacated of fuel, the bottom valve is closed and the hopper is vented to atmospheric pressure. As a final step, the top valve is once again opened to enable feeding. Continuous feeding of biomass into pressure can be achieved by repeating this sequence. If multiple lock hopper systems are operated in parallel, the vent gas of one lock hopper can be used for partial pressurisation of another, thereby reducing the loss of inert gas. The inert gas consumption of a single lock hopper system was reported to be 50 % higher than that for a double system [2].

In a commercial plant, three parallel fuel feeding lines are required to enable continuous gasifier output without interruptions [10]. Common problems related to lock hopper systems include sticking valves, fuel bridging and the relatively high inert gas consumption per unit of energy fed into the process. However, an ample supply of inert $CO_2$ and $N_2$ are available for this from the plant's acid gas removal and air separation units.

## Biomass gasification

Gasification is a thermochemical conversion process that turns carbonaceous feedstocks into a gas mixture rich in carbon monoxide and hydrogen, called product gas or synthesis gas depending on the end-use application. Other major compounds include carbon dioxide, nitrogen, water, methane and a rich spectrum of hydrocarbons and tars. A general objective of gasification is to maximise the yields of light combustible gases and minimise the amounts of condensable hydrocarbons and unreacted char. The exact composition of product gas depends on the type of process feeds, their feed ratios, process parameters and the type of gasification reactor used. In contrast to coal gasification, where char gasification reactions determine the overall yield, in biomass gasification the devolatilisation stage of the feedstock and secondary reactions of primary pyrolysis products play the major role [19]. On a conceptual level, the performance of a gasification process can be measured by calculating its cold gas efficiency (CGE), defined by the following equation:

$$CGE = \frac{(\dot{m} * H)_{\text{syngas}}}{(\dot{m} * H)_{\text{biomass}}}, \tag{1}$$

where $\dot{m}$ represents mass flow and $H$ the lower heating value.[1]

Several types of gasification reactors have been developed in the past, but fluidised-bed reactors have been identified as a reliable and practical solution for large-scale gasification of solid lignocellulosic biomass. In autothermal (directly heated) gasifiers all the reactions take place inside a single reactor whereas in allothermal (indirectly heated) gasifiers the heat generating reactions are separated from the rest of the process and only heat is transferred (normally via circulating bed material) to the gasification reactor. Figure 2 illustrates typical layouts for the two main fluidised-bed biomass gasifier variants. Because in direct gasification all feeds exit the gasifier from a single outlet, the production of nitrogen-free syngas necessitates the use nitrogen-free feed gases. In contrast, the indirectly heated gasifier design makes it possible to produce nitrogen-free syngas also with air as the oxygen-carrier medium, as flue gas from oxidation leaves the gasifier via a separate outlet.

For all gasifier designs, the reactors are fluidised from the bottom through a distributor plate by air, steam or steam and oxygen while feedstock, bed material and additives are fed from the side to the lower part of the reactor. Special bed materials can be used to prevent bed agglomeration, otherwise caused by alkali metals of the biomass feedstock [20].

The autothermal gasifier design can be realised either as a circulating or bubbling fluidised-bed reactor. A few important differences exist between these two reactor types. In a bubbling fluidised-bed (BFB) gasifier, biomass is fed directly into the dense bed where it dries and pyrolyses, causing bed material, steam and oxygen to be in contact with the primary pyrolysis products. In a circulating fluidised-bed (CFB) gasifier, biomass is fed above the dense region to an upward flowing circulation where drying and pyrolysis take place before fuel particles drop to the dense region at the bottom. At the top of the reactor the circulating bed material and unconverted feedstock are separated from gases by a cyclone and returned back to the bottom via a return pipe. Consequently, bed material, steam and oxygen now primarily meet with residual carbon in the dense bed causing it to be converted not only by (relatively slow) char gasification reactions, but by oxidation as well.

## Hot filtration

Filters are used to separate particulates from the gasifier effluent to prevent erosion and fouling of downstream units. In addition to particulates removal, filtration has a significant role in controlling the alkali, heavy metal and chloride removal. Chlorine reacts with calcium and alkali metals to form solid chlorides that can be removed by filtration. Although some of the alkali and heavy metals are in vapour phase under typical gasification conditions, they too can be removed if condensed by cooling down the gas before filtration.

The most challenging aspect in the filtration of biomass-derived gas is related to the behaviour of tars. At lower temperatures (~below 350 °C) tars condense in the dust cake, making the dust sticky and causing poor detachment of the cake by reverse-flow pulse cleaning. At higher temperatures (above ~600 °C) tars

[1] For biomass, values at 50 wt% moisture are used throughout the work.

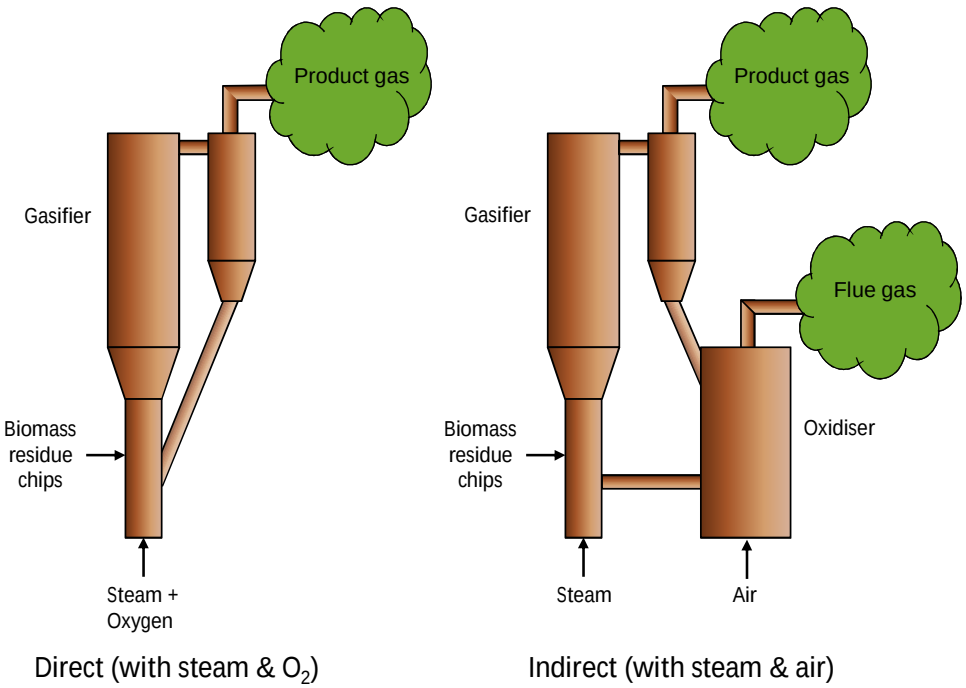


Figure 2: Autothermal (direct) and allothermal (indirect) fluidised-bed gasifiers.

induce filter blinding by forming a sticky, soot-containing cake on the filter surface which again cannot be fully regenerated by pulse cleaning [21, 22]. The most likely reason for this latter phenomenon is the tendency of tar components to crack, polymerise or condense and form soot on the filter. These soot particles can partially enter the filter pores and block them. The blinding effect has also been found to intensify with low dust content. However, stable filter operation has been obtained at 500 - 600 °C [21] and 550 °C is therefore used as a design temperature in many of the analyses presented in this work.

The impact of filtration temperature on the overall feasiblity of synthetic biofuels production has been acknowledged, and developing solutions that allow stable operation at higher temperatures is a major target for hot-gas cleaning R&D. Simeone et al. [23, 24] have performed filtration tests at around 800 °C in steam-$O_2$ gasification conditions with different bed material (magnesite, olivine) and biomass feedstock (wood, miscanthus, straw) combinations. These results also confirmed that the selection of bed material/fuel combination plays an important role in filter performance as they influence the gas quality, especially tars, and dust load in the gas as well as the carry-over of bed material to the filter. Filtration development is an ongoing activity, and a lot of experience has been accumulated at VTT in hot-gas filtration of biomass-derived gasification gas with varying tar loads and different filter media such as ceramic and metallic filters [19, 21, 22, 25–30]. There is also ongoing development of catalytically activated filter elements that would be suitable for simultaneous removal of tars and particulates from biomass-based gasification gas at high temperature [31–42].

## Catalytic reforming

The clean-up of tars from biomass gasification gas has been a topic of numerous R&D projects for decades and has led to two feasible approaches: (1) scrubbing with organic solvents [43, 44] and (2) catalytic reforming [45–50]. Of these, catalytic reforming is particularly suitable for synthesis gas applications because it also handles the non-condensable hydrocarbons and converts organic sulphur species to hydrogen sulphide, a more readily removable form of sulphur for the downstream equipment. The R&D work on catalytic tar reforming started at VTT in the late 1980s and led to the first commercial-scale process designs using catalytic reformers for tar removal in the Skive and Kokemäki CHP plants in the early 2000s [51, 52].

Successful operation of a reformer requires finding the right balance between carbon formation (coking),

temperature and reactor design that maximise the conversion of methane. As described in VTT patents [53–55], a working solution has been found to be a staged configuration where the first stage is based on zirconia and the following stages on precious metal and/or nickel catalysts. The zirconia catalysts are first used to selectively oxidise heavy tars and thus decrease the risk for coking in the reformer [56–58]. The precious metal layer then continues to decompose hydrocarbons and together with the zirconia layer enables the use of high temperatures in the final stages where nickel catalyst layers can be used for methane reforming without problems caused by coking or soot.

The plant configurations created for this work are based on the above-described multistage design where the catalytic reformer is operated downstream from filtration at a temperature range of 850-1000 °C as measured at the reformer's exit. The reformer is operated autothermally with oxygen and steam and is assumed to achieve complete conversion of tars and near-complete conversion of light hydrocarbons.

## Syngas conditioning

After reforming, the properties of the gas are comparable to synthesis gas produced by steam reforming of natural gas. As a result, much of the downstream process can readily be adapted from the synthesis gas industry using commercial equipment and process units, which are described in the following paragraphs.

### CO shifting and sulphur hydrolysis

During reforming, the $H_2/CO$ ratio of the synthesis gas approaches equilibrium[2] being about 1.4 at the reformer exit. This needs to be adjusted to meet the stoichiometric requirement of the fuel synthesis, where the $H_2/CO$ ratio in the fresh feed needs to be in the range of 1-3 depending on the desired product.

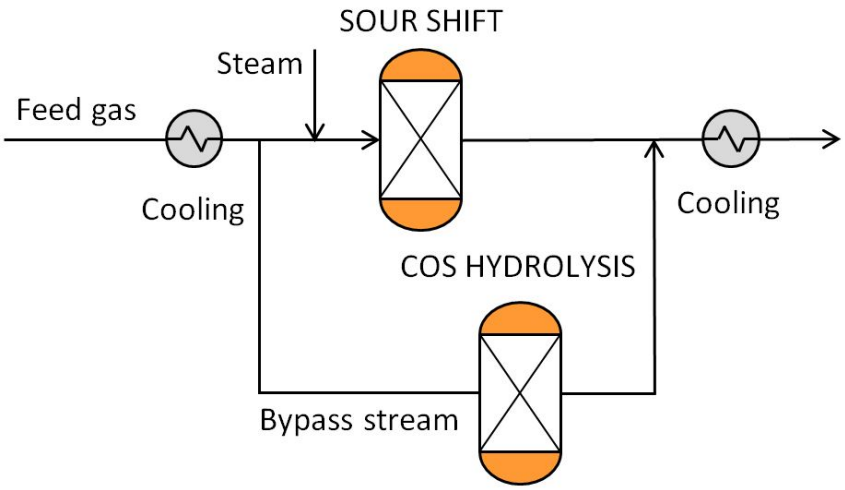


Figure 3: Schematic illustration of a CO shift arrangement.

The adjustment can be carried out by catalysing water-gas shift reaction (2) further in a reactor filled with sulphur-tolerant cobalt catalyst. To drive the reaction and to suppress catalyst deactivation, steam needs to be added until a minimum steam/CO ratio of 1.8 is achieved at the shift reactor's inlet. In an adiabatic reactor, heat release from the exothermic shift reaction gives rise to an ascending temperature profile along the reactor. To prevent deactivation of the catalyst, the outlet temperature needs to be limited to 404 °C [59]. This can be controlled by adjusting the inlet temperature using a syngas cooler that cools down hot syngas exiting the reformer while recovering sensible heat for steam generation.

$$CO + H_2O = H_2 + CO_2 \quad \Delta H_{298\ \mathrm{K},\ 5\ \mathrm{MPa}} = -49.8\ \mathrm{kJ/mol}, \tag{2}$$

[2] Caused primarily by additional residence time in elevated temperatures and the fact that nickel and noble metal catalysts also have activity for the water-gas shift reaction.

In order to avoid an excess amount of CO shift, a portion of the feed gas is bypassed around the reactor (see Fig. 3). The amount of bypass is adjusted to achieve a desired $H_2/CO$ ratio after the gas streams are once again combined. In addition to the CO conversion, the sour shift catalysts also convert carbonyl sulphide (COS), hydrogen cyanide (HCN) and other organic sulphur species to hydrogen sulphide ($H_2S$). To ensure complete hydrolysis of sulphur species, the bypass stream needs to be equipped with a separate hydrolysis reactor. In the CO shift converter the hydrogenation of COS proceeds in parallel with the water-gas reaction according to equation (3), while in the separate reactor the COS hydrolysis follows equation (4) [60]. Both reactions approach the equilibrium well with satisfactory space velocities over modern catalysts.

$$H_2 + COS = H_2S + CO \tag{3}$$

$$COS + H_2O = H_2S + CO_2 \tag{4}$$

**Cooling with heat recovery**

Several heat exchangers are used in this work to transfer heat between process streams. In the modelling of heat exchangers the heat loss is assumed to be 1 % of heat transferred while pressure drop over the heat exchangers is assumed to be 2 % of the inlet pressure. In addition, 15 °C (gas-liq) and 30 °C (gas-gas) temperature differences are used depending on the process streams.

Heat is recovered from syngas with the following placement of coolers: The first evaporator is placed between the gasifier and the filter where the dust-containing syngas is cooled. The superheater is situated right after the reformer, and is followed by a second evaporator in parallel with the first one. Syngas is then cooled down to 200°C with an economiser. The last cooling step from 200 °C to 40 °C is carried out in a two-stage water scrubber to avoid the risk of residual tar condensation on syngas cooler surfaces. The first scrubber unit recovers heat between 200-60 °C and is used to produce district heat. The second scrubber stage lowers temperature further down to about 30 - 40 °C (depending on the temperature of the cooling water) and the recovered heat is transferred to a nearby lake or sea.[3] Any ammonia contained in the gas will be removed by the scrubber. A portion of scrubber water is continuously sent to an on-site water treatment facility, where it is cleaned and used to produce make-up water for the steam system. Formic acid can occasionally be rationed to the scrubber to control the pH value of the washing solution.

**Compression and acid gas removal**

Modern synthesis catalysts are very sensitive to impurities and especially all sulphur species must be removed upstream to a single digit $ppm_v$ level to avoid catalyst poisoning and deactivation. In addition to sulphur, an upstream removal of $CO_2$ from syngas will increase productivity of the synthesis. For the removal of these so called 'acid-gases', physical washing processes using organic solvents can be applied. As these processes operate more efficiently at higher pressure, the feed gas stream is normally compressed before treatment to guarantee sufficient removal of $CO_2$. The molecular mass of the $CO_2$-rich feed gas is normally high enough to enable the use of relatively inexpensive centrifugal compressors for pressurisation. The absorption capacity of solvents for acid gases also increase as the temperature is lowered. Thus, the removal processes are usually operated at the lowest possible temperature [61]. Minor impurities such as carbonyl sulphide, carbon disulphide and mercaptans are fairly soluble in most organic solvents and are to a large extent removed together with $CO_2$ and $H_2S$. The solubilities of hydrocarbons to organic solvents increase with their molecular mass but hydrocarbons above ethane can be to a large extent removed and flashed from the solvent together with acid gases. However, aromatic hydrocarbons are difficult to deal with as they are strongly absorbed by most solvents. They have a tendency to accumulate in the solvent and require a special step to be separated from it [61].

Most organic solvents have much higher solubility for $H_2S$ than for $CO_2$ and therefore it is possible to carry out a selective removal of hydrogen sulphide to a certain degree by adapting the solvent flow rate to the solubility coefficients of the gas components. Co-removal of $CO_2$ and sulphur species can be carried

[3] Or to cooling towers if no natural source of cooling water is available.

out in a single absorber column, while a separate removal of $CO_2$ and $H_2S$ requires a two-column design where each species is removed in separate columns. Both designs enable virtually any $CO_2$ removal rate (depending on pressure, column height, solvent flow rate, temperature etc.) while at the same time removing nearly all sulphur species.

The selective removal of sulphur is relevant especially when treating biomass-derived syntheses gases, which are characterised by a high $CO_2/H_2S$ ratio that complicates subsequent treatment of sulphur. By selectively removing first all of the $H_2S$ and only a portion of $CO_2$, the sulphur stream is more concentrated, and conventional sulphur post-processing becomes possible.

In coal gasification applications the separated $H_2S$ is usually sent to a Claus plant where it is converted to elemental sulphur and sold as a valuable by-product. However, gasification of clean biomass produces too little sulphur for this process to be economically feasible. Therefore, possible options for sulphur processing are conversion to sulphur oxides via combustion or treatment using the Wet Sulphuric Acid (WSA) process.

The basic flow schemes for physical washing processes are simple: For the bulk removal of $CO_2$ only an absorption stage and solvent regeneration by flashing at successively decreasing pressure levels to atmospheric pressure or vacuum is required. However, this approach is applicable only if $H_2S$ is present at very low concentrations. Where $H_2S$ is present in significant amounts, thermal regeneration is usually necessary to reach stringent $H_2S$ purity requirements [61, 62].

Following the physical removal process, catalytic absorbents – called guard beds – are generally used to protect the downstream synthesis catalysts from poisoning by removing the residual amounts of sulphur from the feed gas. The catalytic sorbents are usually single-use fixed-bed solid catalysts that react with $H_2S$ to remove it from the gas stream. A common absorbent is zinc oxide that is capable of bringing the sulphur concentration down to a level around 0.005 $ppm_v$ [63]. It reacts with hydrogen sulphide according to the following reaction:

$$ZnO + H_2S = ZnS + H_2O. \tag{5}$$

The zinc sorbent can not be regenerated and must therefore be landfilled after use. As a result, this option quickly becomes uneconomical due to the cost of zinc as the amount of sulphur species rise to the two digits $ppm_v$ level. As a practical requirement, sulphur concentration in the guard bed feed gas should be low enough to avoid changing of the beds outside scheduled turnarounds.

## Synthesis gas conversion

A synthesis island is a combination of process equipment that convert synthesis gas to desired products at an elevated pressure and temperature in the presence of a catalyst. The system can be divided into synthesis loop, product recovery and upgrading steps. In the synthesis loop, carbon monoxide and hydrogen are converted into the desired product(s) by catalysing the wanted and suppressing the unwanted reactions. The amount of synthesis gas that can be converted to product(s) in a single pass of gas through the reactor depends on the composition of the fresh feed, selection of catalyst and design and size of the reactor. Recycling of unconverted synthesis gas back to the upstream process makes it possible to convert a larger fraction of biomass energy to synthetic fuel. Although the recycle design enables high overall conversion, it increases gas flows within the recycle, necessitates a feed/effluent heat exchanger and requires a recirculator (compressor) to counter pressure losses in the loop.

Gases such as methane, argon and nitrogen are considered inerts in the synthesis loop and their build-up needs to be controlled by continuously purging part of the recycle flow. The concentration of these inerts should be minimised already in the upstream process as higher amounts of inerts lead to increased purge gas volumes in the synthesis loop thus having an adverse effect on the economics.

The catalytic reactions are associated with a substantial release of heat as by-product. Typical liquid fuel syntheses operate in the range of 200-300 °C[4], and the released reaction heat can thus be recovered by raising saturated steam in the range of 15-85 bar.

[4] High temperature methanation being a notable departure from this.

The focus in syntheses designs for this work has been on minimising specific synthesis gas consumption in the conversion loop as it is expect to provide favourable economics due to reduced feedstock costs together with investment savings in the upstream process due to lower gas volumes. This objective is achieved by maximising synthesis gas efficiency $\eta_{sg}$

$$\eta_{sg} = 1 - \frac{(CO + H_2)_{\text{in purge}}}{(CO + H_2)_{\text{in fresh feed}}}, \tag{6}$$

where CO and $H_2$ refer to the molar flows of these components in the gas. In most cases the bulk of the formed product is recoverable from the reactor effluent (at synthesis pressure) simply by condensation with cooling water at 20-45 °C. The design of an upgrading area is highly dependent on the product being produced and ranges from a simple distillation approach to a full-blown refinery employing hydrocrackers and treaters. These issues are discussed further in the appropriate sections.

## Synthesis of methane

Conversion of carbon oxides and hydrogen to methane over catalysts based on nickel and other metals (Ru, Rh, Pt, Fe and Co) was first discovered in 1902 by Sabatier and Senderens [64]. The process of methanation can be described with the water-gas shift (2) and the following reactions:

$$CO + 3H_2 = CH_4 + H_2O \quad \Delta H = -206 \text{ kJ/mol}, \tag{7}$$

$$CO_2 + 4H_2 = CH_4 + 2H_2O \quad \Delta H = -165 \text{ kJ/mol}. \tag{8}$$

As both reactions are exothermic and accompanied by a net decrease in molar volume, the equilibrium is favoured by high pressure and low temperature. Although many metals are suitable for catalysing these reactions, all commercially available modern catalyst systems are based on nickel due to its favourable combination of selectivity, activity and price [65]. Technology for the production of synthetic methane (also called Synthetic Natural Gas, SNG) from lignite and coal was intensively studied through the 1960s and 1970s in the United States, Germany and Great Britain. This development resulted in a few pilot and demonstration plants, but only one commercial-scale installation: the Great Plains Synfuels Plant commissioned in 1984 (North Dakota, USA) [66]. Recently, a plant producing methane from solid biomass feedstocks was inaugurated in Gothenburg, Sweden. The official start-up of this 20 $MW_{th}$ facility was in October 2013 and once fully operational, it will be the world's first plant that produces biomethane via gasification. The biomethane will be injected to the Sweden's natural gas grid and will be used for vehicle fuel, feedstock for process industry and fuel for CHP or heat production [67].

### Synthesis design

Controlling the release of heat during methanation is a major concern for an SNG process design. Efficient heat management is required to minimise catalyst deactivation by thermal stress and maximise methane yield by avoiding equilibrium limitations. In practise, two main reactor concepts have proven suitable for reliable execution of catalytic methanation: (1) fluidised-bed reactors and (2) series of adiabatic fixed-bed reactors using either intermediate cooling or gas recycle, although only the latter has been utilised for industrial operation [68].

The simulation model developed for this work is based on the fixed-bed concept and inspired by the high temperature methanation process 'TREMP', developed and offered by Haldor Topsøe [69]. A simplified layout of the high-temperature methanation design is given in Fig. 4. It features six adiabatic fixed-bed reactors connected in series and equipped with intercoolers. The pressure at the inlet of the first reactor is 15 bar. The inlet syngas is mixed with recycle gas and preheated to 300 °C. The amount of recycling is chosen to limit temperature increase in the first reactor to 700 °C. Due to the high temperature window in the first reactor, special catalysts are needed that combine good low-temperature activity with high-temperature stability [68]. The hot effluent exiting from the first four reactors is cooled to 300 °C before entering the next reactor in the series. Effluent from the fifth reactor is cooled down to condense and separate the by-product water before being fed to the last reactor. Overall extent of syngas conversion to

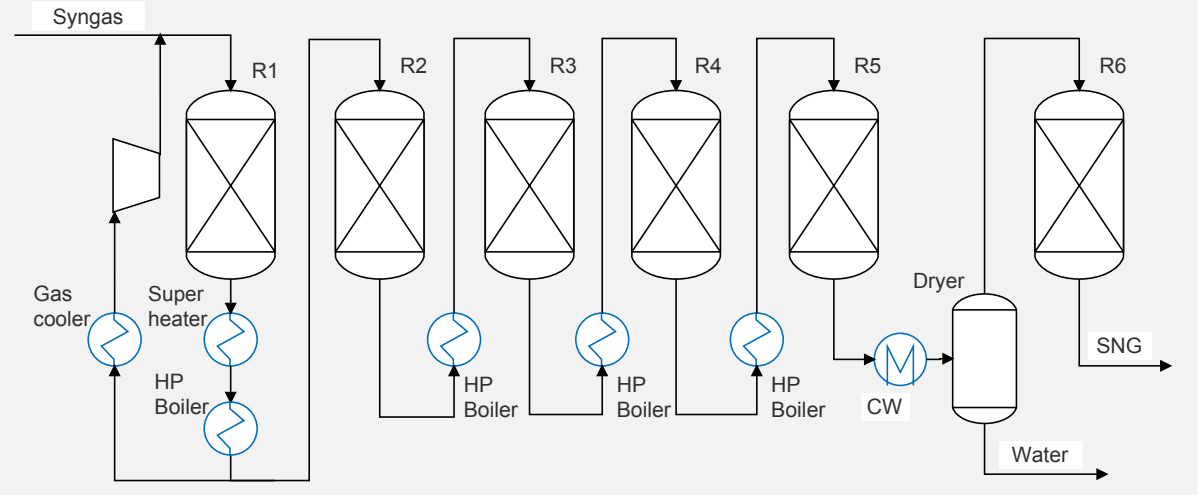


Figure 4: Simplified layout for the high-temperature methanation section.

methane is >99.5 % and the effluent exits the system at 11 bar pressure. Equilibrium conversions in the reactors are calculated with Aspen using the Soave-Redlich-Kwong (SRK) equation of state model. The recovered heat is used to produce high-pressure superheated steam for the plant's steam cycle.

### Product recovery and upgrade design

When the synthesis product is liquid, it can be conveniently recovered from unconverted gases of the reactor's effluent by means of condensation. However, in methanation the main product is gaseous and such separation is not possible. Therefore, to achieve high-methane-content SNG product, the amount of inert gases (nitrogen, argon, etc.) needs to be minimised along the production chain. The quality of the SNG product can be estimated by calculating its Wobbe index, $I_W$, defined as

$$I_W = \frac{\Delta H_v}{\sqrt{\rho/\rho_0}}, \tag{9}$$

where $\Delta H_v$ is the higher heating value of the SNG product, $\rho$ the density of SNG under standard conditions (STP) and $\rho_0$ the density of dry air at STP. The $I_W$ is a measure of the interchangeability of different fuel gases[5] and when equal Wobbe indices are reached, distribution of SNG within the natural gas infrastructure can be executed without problems to end-users. Typical $I_W$ values for natural gas range from 45.7 to 54.7 MJ/Nm$^3$ [70]. For countries where natural gas has high energy content, some propane addition might be needed to reach the required Wobbe index for the product.[6]

The produced SNG also needs to be pressurised to enable distribution within the existing natural gas infrastructure. As the required level of compression differs among countries and applications, compression of the SNG product to any specific pressure is not considered in the analysis presented in this work. However, it is acknowledged that in vehicle use gas tanks are usually designed to operate up to 200 bar pressure, a fairly uniform standard.

## Synthesis of methanol

The production of methanol (MeOH) from synthesis gas was first described by Patart [71] and soon after produced by BASF chemists in Leuna, Germany in 1923 [72]. This became possible through the

[5] When two fuels have identical Wobbe indices they will release the same amount of energy during combustion at a given pressure.

[6] For example, Sweden is supplied with Danish natural gas that is characterized by a high methane content. Therefore, propane needs to be added to biomethane to match the Wobbe index of the natural gas [70].

development of sulphur- and chlorine-resistant zinc oxide ($ZnO - Cr_2O_3$) catalyst that benefitted from the engineering knowhow acquired from the prior development of ammonia synthesis technology [73]. The main shortcoming of this process was the low activity of the catalyst, which required the use of relatively high reaction temperatures in the range of 300-400 °C. As a result, a high (about 350 bar) pressure was also needed to reach reasonable equilibrium conversions [74]. Despite the drawbacks, high pressure methanol synthesis was the principal industrial production route of methanol for 40 years. In the 1960s workers at ICI pioneered an improved process using more active and highly selective copper oxide catalyst, which became a practical option through the advent of virtually sulphur-free ($H_2S <$ 0.1 ppm) synthesis gas produced by natural gas steam reformers. This low-pressure methanol synthesis, operated at 250-280 °C and 60-80 bar has since become the exclusive production process for industrial-scale methanol with the largest plants having a capacity of more than 5000 metric tons per day (MTPD) [75, 76].

All commercially available modern methanol catalysts are based on $Cu$-$ZnO$-$Al_2O_3$ or $Cr_2O_3$ with different additives and promoters. These catalysts allow the production of methanol at over 99.9% selectivity with higher alcohols, ethers, esters, hydrocarbons and ketones as primary by-products. In addition to the water-gas shift reaction (2), methanol synthesis can be described with the following reactions [77]

$$CO + 2H_2 = CH_3OH \ \Delta H_{25^\circ\mathrm{C}} = -90.9 \text{ kJ/mol}, \tag{10}$$

$$CO_2 + 3H_2 = CH_3OH + H_2O \ \Delta H_{25^\circ\mathrm{C}} = -50.1 \text{ kJ/mol}. \tag{11}$$

The kinetics and mechanisms of methanol synthesis have been discussed since the beginning of methanol research. An enduring question has been whether the formation of methanol proceeds primarily via CO or $CO_2$ hydrogenation; some authors have reported a sharp maximum of the reaction rate for $CO_2$ contents in the range of 2-5%, while others have reported a constant increase with increasing $CO_2$ content [76]. According to Hansen [78], there is an array of evidence favouring the $CO_2$ route to methanol and only a few proponents still believe that methanol is formed from CO in any substantial quantities, at least with industrial catalysts and conditions.

As both methanol reactions are exothermic and accompanied by a net decrease in molar volume, the equilibrium is favoured by high pressure and low temperature. However, the copper-based catalyst is not active at temperatures much lower than 220 °C and a compromise between reaction kinetics and equilibrium considerations is required [77]. Methanol synthesis is characterised by the ratio ($H_2$ - $CO_2$)/(CO + $CO_2$), where $H_2$, CO and $CO_2$ represent their respective concentrations in the fresh feed that is continuously fed to the synthesis loop. This ratio, often referred to as the module $M$, should equal 2.03 for an ideal composition of fresh feed to synthesis [79]. Typical inerts in the MeOH synthesis are methane, argon and nitrogen [79].

**Synthesis design**

Several different basic designs for methanol converters have been proposed since the start of production on an industrial scale in the 1960s [76]. Design of the methanol loop in this work is based on a quasi-isothermal tubular reactor where synthesis gas flows axially through the tubes filled with catalysts and surrounded by boiling water. The reaction heat is continuously removed from the reactor to maintain essentially isothermal conditions at 250 °C and 80 bar by controlling the pressure of the steam drum. The reaction temperature needs to be kept low to ensure favourable equilibrium conditions and to prevent loss of catalyst activity caused by sintering of the copper crystallites.

Boiling-water reactors are easy to control and they approach the optimum reaction rate trajectory well. However, the design itself is complicated and the maximum single line capacity is constrained to about 1800 metric tonnes per day, due to the tube sheet that restrains reactor diameter to around 6 m [78]. The equilibrium conversions in the methanol converter is calculated with Aspen Plus using the Soave-Redlich-Kwong (SRK) equation of state model, which has been found to give better agreement with experimental findings than the Peng-Robinson equation of state, the virial equation, the Redlich-Kwong equation or Lewis and Randall's rule [78].

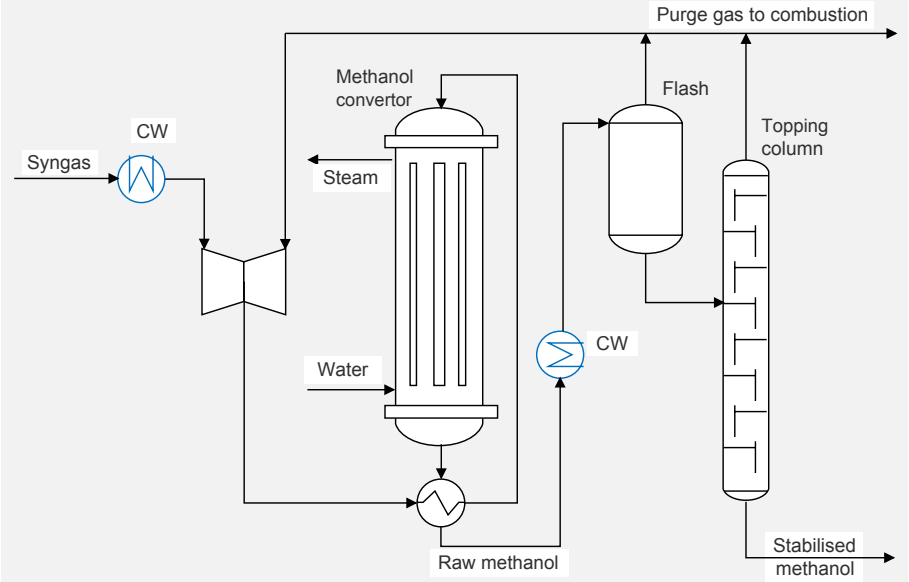


Figure 5: Simplified layout for the low-pressure methanol synthesis loop, product recovery and 'low-grade' distillation section.

A simplified layout of the methanol loop design is given in Fig. 5. The compressed fresh feed ('make-up') is first mixed with unconverted recycle gas and preheated in a feed/effluent heat exchanger before feeding to the methanol converter. As the per-pass conversion of reactants to methanol is limited by equilibrium, a substantial amount of unconverted gas still exists at the reactor outlet and needs to be recycled back to the reactor to boost overall conversion. The pressure drop across the methanol loop is set to 5 bar.

### Product recovery and upgrade design

After the reactor, effluent is cooled against the feed stream in a feed/effluent heat exchanger followed by further cooling with water to separate raw methanol product from unconverted gases by means of condensation. The unconverted gases are recompressed and recycled back to the reactor while the condensed crude methanol is sent to further purification.

The raw methanol contains also water that was formed as a by-product of $CO_2$ conversion. For carbon-rich syngas, the desired $M$ can be achieved with minimal $CO_2$ content in the fresh feed, leading to limited by-product water formation and thus reducing the amount of energy needed for distillation.

Two generally accepted product quality standards exist for methanol: fuel-grade and chemical-grade; designated according to the use for which they are destined. The requirements for fuel-grade[7] methanol are less stringent than those for chemical-grade methanol. In cases where even lower qualities can be tolerated, like subsequent conversion to gasoline or olefins, individual specifications can be agreed between the user and producer [73]. Higher purities can be achieved simply by adding more distillation columns, which contributes to additional capital and energy costs. For example, energy consumption for the production of fuel-grade methanol is only one third of that needed for chemical-grade methanol [73].

For the purpose of this analysis, a one column separation design was adopted where light ends (ethers, ketones and aldehydes) and any dissolved gases like hydrogen, carbon oxides, methane and nitrogen are removed from the overhead of an atmospheric column having 80 trays. The bottom product, called stabilised methanol, has a methanol content of 98.5 vol%, the balance being essentially water, and is stored in offsite tanks.

The column is simulated with Aspen Plus using the Non-Random Two-Liquid (NRTL) activity coefficient model [80]. For this 'low-grade' design, the recovery of waste heat provides the needed utilities for the

[7] The main criteria for fuel-grade methanol are that it doesn't contain any dissolved gases or low-boiling substances (such as dimethyl ether) and that the water content is below 500 wt-ppm [73].

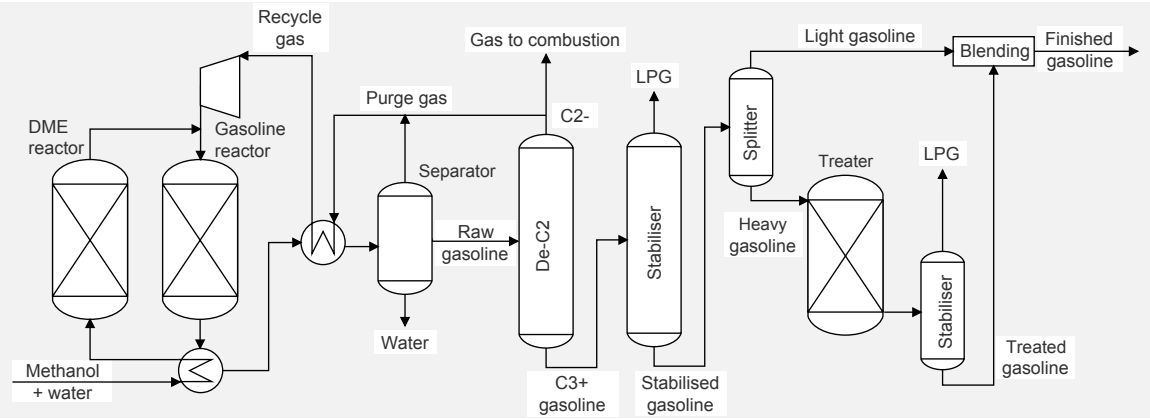


Figure 6: Simplified layout for the two-step gasoline synthesis, product recovery and distillation section, adapted from [89].

upgrading, leading to zero net parasitic utilities demand for the area.

## Synthesis of gasoline

The most significant development in synthetic fuels technology since the discovery of the Fischer-Tropsch process has been the development of methanol-to-gasoline (MTG) synthesis by Mobil in the 1970's [81–83]. Both processes enable the production of liquid hydrocarbons from carbonaceous feedstocks that can be used as drop-in replacements for conventional petroleum fuels. However, in contrast to the FT process that produces an array of hydrocarbons at a wide carbon number range, gasoline synthesis is very selective, producing primarily finished gasoline blendstock and a by-product stream that resembles liquefied petroleum gas (LPG).

The production of synthetic gasoline is a two-step process that involves 1) production of oxygenates from synthesis gas and 2) subsequent conversion of oxygenates to higher hydrocarbons boiling in the gasoline range [84]. These processes may be carried out as separate steps using methanol as the intermediate oxygenate, or in integrated fashion by producing a methanol/dimethyl ether mixture directly from syngas that is conveyed in its entirety to a downstream gasoline converter [85]. A simplified layout of the design adopted for this work is shown in Fig. 6.

The conversion of methanol to gasoline proceeds essentially according to the reaction

$$CH_3OH \rightarrow (CH_2) + H_2O, \tag{12}$$

while dimethyl ether is converted according to

$$CH_3OCH_3 \rightarrow (CH_2)_2 + H_2O. \tag{13}$$

In these reaction equations, $(CH_2)$ represents the paraffinic and aromatic hydrocarbons that are produced in the gasoline synthesis step [86]. A more detailed discussion on the reaction mechanisms is available in Ref. [82]. The conversion of oxygenates into $C_2$-$C_{10}$ hydrocarbons is catalysed by zeolites such as ZSM-5 that have a silica to alumina mole ratio of at least 12 and a pore size defined by 10 membered rings. The manufacture of these zeolites is well known and commercial catalysts are available [87]. A unique characteristic of the gasoline product is the abrupt termination in carbon number at around $C_{10}$ due to the shape-selective nature of the zeolite catalyst. As a result, the composition and properties of the $C_{5+}$ fraction are those of a typical high-quality aromatic gasoline, boiling in the 120-200 °C range [83, 88].

One disadvantage of synthetic gasoline is its relatively high (3-6 wt%) durene content in comparison to conventional (0.2-0.3 wt%) gasoline. Although durene has a good octane number and it boils within the

Table 3: MTG yield structure for a fixed-bed reactor given per kg of pure methanol input to a DME reactor [6].

| **Component name** | **Formula** | **Molar mass** | **kmol/kgMeOH** |
|---|---|---|---|
| Hydrogen | $H_2$ | 2.02 | 0.00001049 |
| Water | $H_2O$ | 18.02 | 0.03137749 |
| Carbon monoxide | CO | 28.01 | 0.00000446 |
| Carbon dioxide | $CO_2$ | 44.01 | 0.00001390 |
| Methane | $CH_4$ | 16.04 | 0.00019586 |
| Ethene | $C_2H_4$ | 28.05 | 0.00000473 |
| Ethane | $C_2H_6$ | 30.07 | 0.00005067 |
| Propene | $C_3H_6$ | 42.08 | 0.00002055 |
| Propane | $C_3H_8$ | 44.10 | 0.00042752 |
| 1-Butene | $C_4H_8$ | 56.11 | 0.00008593 |
| n-Butane | $C_4H_{10}$ | 58.12 | 0.00019381 |
| i-Butane | $C_4H_{10}$ | 58.12 | 0.00062811 |
| Cyclopentane | $C_5H_{10}$ | 70.13 | 0.00001514 |
| 1-Pentene | $C_5H_{10}$ | 70.13 | 0.00014015 |
| N-pentane | $C_5H_{12}$ | 72.15 | 0.00008633 |
| I-pentane | $C_5H_{12}$ | 72.15 | 0.00075797 |
| Gasoline* | $C_7H_{16}$ | 100.2 | 0.00283472 |

*Gasoline is assumed to be represented as n-heptane ($C_7H_{16}$)

gasoline boiling range, it has a high melting point (79 °C) which is known to cause carburettor "icing" if the gasoline durene concentration is too high. To eliminate this problem, the content of durene should be reduced to under 2 wt% [90].

In addition to ExxonMobil, Haldor Topsøe has developed a gasoline process called Topsøe Integrated Gasoline Synthesis (TIGAS). The key distinction from ExxonMobil's MTG technology is that in TIGAS the synthesis gas is converted directly to a mixture of DME and methanol, followed by conversion to gasoline in a downstream reactor thus making upstream production and intermediate storage of methanol unnecessary [91].

### Synthesis design

The synthesis design is based on the conventional two-step gasoline process, where methanol is produced first and then stored until subsequent conversion to gasoline that might or might not take place at the same site as the manufacture of methanol. In the design, methanol is first pumped to 22.7 bar and then vaporised and superheated to 297 °C in heat exchange with the hot reactor effluent. The methanol is then fed to an adiabatic fixed-bed dehydration (DME) reactor where it is converted to an equilibrium mixture of methanol, DME and water. The effluent exits the reactor at 409 °C and 21.7 bar and is admixed with recycle gas and fed to a second reactor where it is converted to gasoline [83]. A large recycle stream is needed to limit the outlet temperature of the adiabatic gasoline reactor to 400 °C. We assume the molar recycle to fresh feed ratio to be 7.5:1 [89]. To control the build-up of inerts in the synthesis loop some gas needs to be purged from the recycle flow, which is then transferred to combustion. The equilibrium conversion of methanol to DME and water is simulated with Aspen Plus using the Soave-Redlich-Kwong (SRK) equation of state model [92].

Due to the proprietary nature of the process, very little information has been published about the performance of the MTG reactor, thus complicating the process simulation effort. However, a RYield block was chosen to simulate gasoline synthesis using the product yield structure of the MTG's gasoline reactor (See Table 3) as reported by Larson et al. [6] based on the work of Barker et al. [93] and Schreiner [94].

### Product recovery and upgrade design

The gasoline reactor effluent is condensed and separated into water, raw gasoline, purge and recycle gas streams. The water phase contains about 0.1-0.2 wt% oxygenates (alcohols, ketones and acids) that can

be treated with conventional biological means to yield an acceptable effluent for discharge [84]. The condensed raw gasoline is sent to a product recovery section where it is fractionated by distillation. The liquid hydrocarbons are first transferred to a de-ethaniser where $C_{2-}$ fraction is separated from the overhead and the bottoms are passed to a stabiliser where a stream of LPG is produced overhead. The stabilised gasoline is sent to a gasoline splitter where it is separated into light and heavy gasoline streams. The heavy gasoline stream undergoes durene treatment (HGT) that includes: isomerisation, disproportionation, transalkylation, ring saturation and dealkylation/cracking reactions. Yield loss of $C_{5+}$ due to the treatment is minimal as only 10 - 15 % of the gasoline needs to be processed [84, 90]. After HGT the treated heavy gasoline is blended with light gasoline and $C_4$'s to produce finished gasoline containing less than 2 wt% durene [84, 90].

The required hydrogen for the durene treatment can be separated from synthesis gas via pressure swing adsorption. However, Larson et al. [6] have estimated that the hydrogen requirement of durene treatment is only 0.2 to 0.6 kg of hydrogen per tonne of total gasoline produced. Due to this minuscule consumption, this step was not included in the simulation. In addition, it is assumed that the recovery of waste heat provides the needed utilities for the upgrading, leading to zero net parasitic utilities demand for the area.

## Oxidiser

Synthesis plants consume varying amounts of electricity depending on the pressure levels of process equipment (compression work) and overall plant design. In the studied thermochemical configurations electricity is produced with a turbine connected to the steam system. Roughly half of the electricity consumption can be generated using steam recovered from syngas cooling. The rest needs to be satisfied with the combination of steam generated by combustion of by-products and purchases from the electricity grid.

Some carbon is always left unconverted in the gasifier and some syngas is left unconverted in the synthesis loop. The filter ash stream of a 100 $MW_{th}$ gasifier having a carbon conversion of 98% corresponds to an energy flow of about 2 $MW_{th}$. This energy can be recovered by combustion of the filter ash (containing about 50/50 carbon/ash) in a suitable boiler (oxidiser). The amount of energy contained in the purge gas varies considerably depending on the type and configuration of the synthesis. If the unconverted gas is separated from the synthesis effluent and recycled back to the reactor inlet, only small amount of gas is eventually left unconverted. Such small purges could be combusted in a boiler together with filter ash, or separately in a gas engine to achieve higher power production efficiency. A further option for larger purge gas streams would be combustion in a gas turbine integrated with the plant steam system.

The saturated steam raised in the synthesis reactor carries substantial amount of enthalpy but little exergy due to its low temperature that limits the amount of work that can be recovered from it. Its value could be greatly increased by superheating in an auxiliary boiler (oxidiser) before injection to turbine, or alternatively it could be used directly as process steam via a pressure let down. An auxiliary boiler also increases the flexibility of plant operation by its ability to produce steam independently from the gasification plant, a convenient attribute during start-ups, process failures, et cetera.

All plant configurations considered in this work feature a bubbling fluidised-bed combustor producing 93.5 bar superheated steam at 500 °C operated with lambda 1.2 and modelled in Aspen as RStoic. For the allothermal configurations heat for the indirect steam gasifier is generated in this oxidiser. The pressure drop over the reactor is set to 0.1 bar, and heat is recovered from flue gas cooling to generate steam and to preheat the combustion air to 250 °C. The outlet temperature of flue gas is 150 °C.

## Steam system

All plant configurations examined in this work feature a back-pressure steam turbine design that co-generates electricity, process steam and district heat (DH). All plant configurations are designed self-sufficient in terms of steam, while electricity is balanced with grid purchases and surplus heat is sold to a nearby district heating network. A simplified layout of the steam cycle is illustrated in Fig. 7.

The effluent from the syngas water scrubber is sent to an on-site water treatment process where it is purified and used to produce make-up water for the steam cycle. The make-up is fed to the feedwater

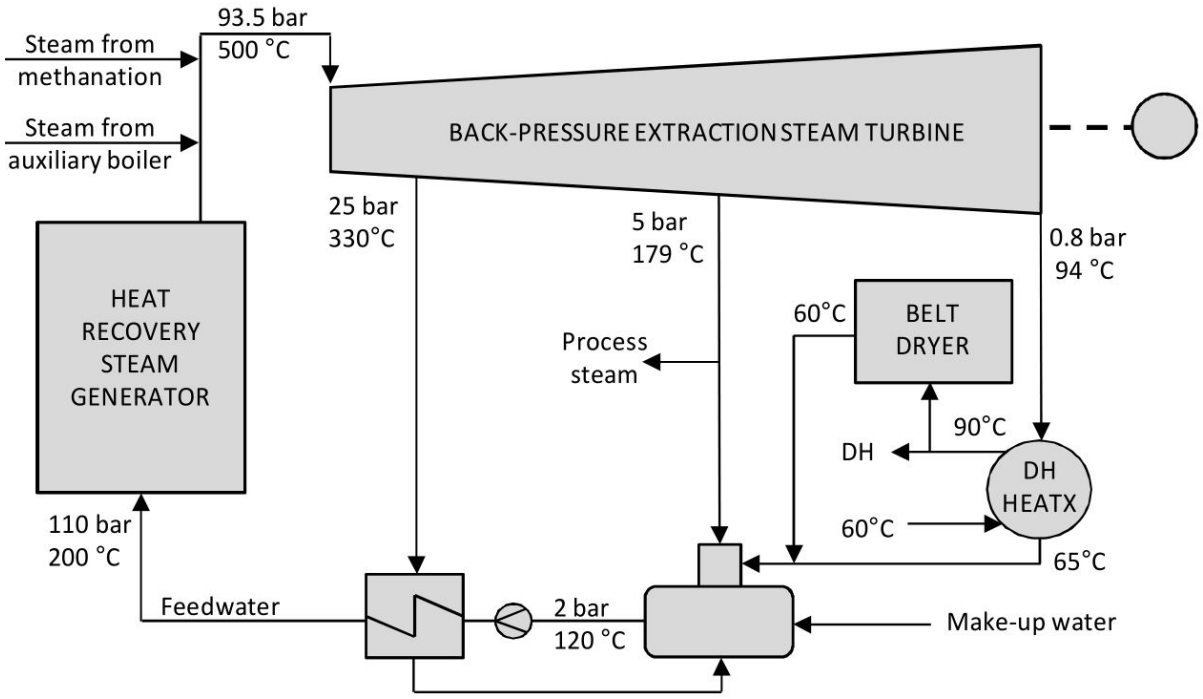


Figure 7: Simplified layout of the steam cycle design.

tank operating at 2 bar and 120 °C and heated with deaeration (process) steam. From the tank the feed water is distributed to the auxiliary boiler, the gasification plant and the synthesis island. To avoid possible residual tar condensation on the cooler surfaces, feed water entering the syngas cooling system is preheated to 200 °C with extraction steam from the turbine.

Steam is generated at several locations in the overall process. The majority is raised by recovering heat from syngas cooling. Additional steam is produced by combusting unconverted carbon from the gasifier (filter dust) and unconverted syngas from the synthesis (if available) in an auxiliary boiler. The live steam parameters are 93.5 bar[8] and 500 °C, which are typical values for a small-scale biomass power plant [95].

In plant designs that feature synthetic natural gas production, the synthesis exotherm is utilised to produce superheated steam that can be used in the turbine as additional live steam. In plant designs that feature methanol production, the synthesis exotherm is utilised to produce saturated steam at 43 MPa and 255 °C that is used to satisfy part of the plant's process steam consumption.

The steam turbine size is approximately 20 $MW_e$ in the studied configurations. Such small turbine is physically limited to a maximum of 4 extraction holes that needs to be considered when designing the steam system [96]. The turbine is modelled as isentropic using the ASME 1967 steam table correlations with following specifications: isentropic efficiency 78 %, generator efficiency 97 % and mechanical efficiency 98 %. The first steam extraction point from the turbine is fixed at 25 bar and 330 °C and used to preheat feedwater to 200 °C. The second extraction point is fixed at 5 bar[9] and 179 °C and used to supply steam for the gasifier, reformer, deaerator and AGR solvent regeneration. The rest of the steam is extracted at the turbine's back-pressure (0.8 bar), condensed and used to produce hot water at 90 °C. The hot water provides heat for drying the wet biomass feed and the rest is sold to a nearby district heating grid.

[8] After 17.5 bar pressure drop mostly caused by superheaters.
[9] 1 bar higher than gasification pressure to allow pressure drop for the inlet valves.

## Cryogenic air separation

When gasification and reforming are based on partial oxidation, pure oxygen is required for the generation of nitrogen-free synthesis gas. Although the investment cost of oxygen production is substantial, it is considered to be offset by the reduced costs of the smaller equipment and more efficient recycle configuration around the synthesis made possible by the absence of nitrogen in the syngas. A variety of processes exist for the separation of oxygen and nitrogen from air (e.g. adsorption processes, polymeric membranes or ion transportation membranes), but for the production of large quantities (>20 tons per day) of oxygen and nitrogen at high recoveries and purities, the conventional multi-column cryogenic distillation process still remains as the most cost-effective option [1].

In the cryogenic air separation unit, air is first pressurised and then purified from $CO_2$ and moisture by a molecular sieve unit. The clean compressed air is then precooled against cold product streams, followed by further cooling down to liquefaction temperature by the Joule-Thompson effect. The liquefied air is then separated to its main components in a distillation tower operating between the boiling points of nitrogen and oxygen (-196 °C to -183 °C). Because the boiling point of argon is very similar to that of oxygen, the purity of the oxygen product from a double column unit is limited to around 96 %. However, when higher purity oxygen is required, argon can be removed by adding a third distillation column that yields a pure argon product [97]. ASU design adopted for this work features a stand-alone cryogenic air separation unit producing 99.5 mol% oxygen at a 1.05 bar delivery pressure.

Cryogenic air separation is an energy-intensive process that requires a substantial amount of power to operate. According to [1] a plant producing 890 tons of oxygen per day at 500 psig (35.5 bar) using a full pumped liquid oxygen cycle consumes about 12.5 MW of electric power. Based on an Aspen simulation, compression of oxygen from 1.05 to 35.5 bar[10] consumes 3.76 $MW_e$. Subtracting this from 12.5 gives 8.7 MW, which yields a specific power consumption of 260 kWh/ton$O_2$ for an ASU delivering oxygen at 1.05 bar pressure.

## Electrolysis of water

Hydrogen can be produced by passing an electric current through two electrodes immersed in water. In the process, water molecules are split to produce oxygen and hydrogen according to the following overall reaction:

$$2H_2O(l) \rightarrow 2H_2(g) + O_2(g). \tag{14}$$

Presently the production of hydrogen via electrolysis is mainly limited to small or special applications, while larger quantities are produced by steam reforming of natural gas or other fossil fuels. The most established and commercially available technology is based on alkaline electrolysers, while proton exchange membrane (PEM) electrolysis and solid oxide electrolysis cells (SOEC) are examples of more advanced and emerging systems [98]. SOEC electrolysers are the most efficient but the least developed. PEM electrolysers are more efficient than alkaline and do not have issues with corrosion or seals as do the SOEC systems, but cost more than alkaline systems. Alkaline electrolysers have the lowest efficiency, but are the most developed and lowest in capital cost [99].

In this work, electrolytic hydrogen is produced via low temperature alkaline water electrolysis.[11] The system is composed of electrodes, a microporous separator, an aqueous solution of water and 25-30 wt% of potassium hydroxide (KOH) as an electrolyte [100]. The liquid electrolyte is not consumed in the reaction, but must be replenished over time to cover losses that occur during hydrogen recovery. Water is decomposed into hydrogen and $OH^-$ in the cathode. The $OH^-$ travels through the electrolytic material to the anode where $O_2$ is formed, while hydrogen is left in the alkaline solution and separated by a gas/liquid separator unit outside the electrolyser cell. Nickel with a catalytic coating, such as platinum, is the most common cathode material, while for the anode nickel or copper metals coated with metal oxides, such as manganese, tungsten or ruthenium are used [99].

[10] Assuming centrifugal compressor having a polytropic efficiency of 87 %, driver efficiency of 92 % and 5 stages with intercooling to 35 °C.

[11] Norsk Hydro's Atmospheric Type No. 5040 (5150 Amp DC).

Commercial systems are typically run with current densities in the range of 100 - 300 mA/cm$^2$. The product hydrogen and oxygen can be assumed to be of 100 % purity due to the very low concentration of contaminants [101].

### Carbon dioxide hydrogenation

Carbon dioxide can be used as a $C_1$ building block for making organic chemicals, materials and fuels [102]. However, it is considered a less favourable feedstock for fuels production than carbon monoxide due to more intensive use of resources (energy, $H_2$, more reaction steps, etc.) [103]. Presently, the use of $CO_2$ as a chemical feedstock is limited to few industrial processes such as urea synthesis and its derivatives, salicylic acid and carbonates [103].

Production of methane from $CO_2$ via Sabatier reaction (8) is a well-known route that can be realised using existing methanation catalysts. In addition, catalysts allowing direct hydrogenation of $CO_2$ to methanol via reaction (11) have been developed, and pilot-scale plants based on this technology demonstrated [104–108]. However, the conversion of pure $CO_2$ into methanol is challenging due to difficulties associated with the chemical activation of $CO_2$ and commercial catalyst systems used for this task have low catalytic activity and greatly reduced yield [109–111]. In addition, almost one third of the input $H_2$ is consumed to produce by-product water.

Despite these challenges, plant configurations developed for this work assume that catalyst systems based on the conversion of $CO_2$ or CO and $CO_2$ mixtures are available and operate close to equilibrium conversion with the same catalyst productivity than commercial alternatives using carbon monoxide as the main feed. This approach is motivated by recent breakthroughs in catalyst development suggesting that the activity of a catalyst in transformation of $CO_2$ to methanol can be greatly improved [112].

## References


[1] A. Smith, J. Klosek, A review of air separation technologies and their integration with energy conversion processes, Fuel Processing Technology 70 (2) (2001) 115–134. doi:10.1016/S0378-3820(01)00131-X.

[2] M. Swanson, M. Musich, D. Schmidt, J. Schultz, Feed system innovation for gasification of locally economical alternative fuels (FIGLEAF) Final report, Tech. rep., U.S. Department of Energy (2002).

[3] I. Hannula, E. Kurkela, A semi-empirical model for pressurised air-blown fluidised-bed gasification of biomass, Bioresource Technology 101 (12).

[4] I. Hannula, E. Kurkela, A parametric modelling study for pressurised steam/$O_2$-blown fluidised-bed gasification of wood with catalytic reforming, Biomass and Bioenergy 38 (2012) 58–67, Overcoming Barriers to Bioenergy: Outcomes of the Bioenergy Network of Excellence 2003-2009. doi:10.1016/j.biombioe.2011.02.045.

[5] G. Liu, E. D. Larson, R. H. Williams, T. G. Kreutz, X. Guo, Supporting information for making Fischer-Tropsch fuels and electricity from coal and biomass: Performance and cost analysis, Energy & Fuels 25 (1). doi:10.1021/ef101184e.

[6] E. Larson, R. Williams, T. Kreutz, I. Hannula, A. Lanzini, G. Liu, Energy, environmental, and economic analyses of design concepts for the co-production of fuels and chemicals with electricity via co-gasification of coal and biomass, Final report under contract DEFE0005373 to the National Energy Technology Laboratory, US Department of Energy, Princeton University (2012).

[7] P. Chiesa, S. Consonni, T. Kreutz, R. Williams, Co-production of hydrogen, electricity and $CO_2$ from coal with commercially ready technology. Part A: Performance and emissions, International Journal of Hydrogen Energy 30 (7) (2005) 747–767. doi:10.1016/j.ijhydene.2004.08.002.

[8] A. Glassman, Users manual for updated computer code for axial-flow compressor conceptual design, Tech. rep., University of Toledo, Toledo, Ohio (1992).

[9] E. D. Larson, H. Jin, F. E. Celik, Large-scale gasification-based coproduction of fuels and electricity from switchgrass, Biofuels, Bioproducts and Biorefining 3 (2) (2009) 174–194. doi:10.1002/bbb.137.
URL 10.1002/bbb.137

[10] BiGPower deliverable 71: Finnish case study report, Project co-funded by the European Commission within the Sixth Framework Programme project no. 019761, Carbona, Inc. (2009).

[11] T. Kreutz, R. Williams, S. Consonni, P. Chiesa, Co-production of hydrogen, electricity and $CO_2$ from coal with commercially ready technology. Part B: Economic analysis, International Journal of Hydrogen Energy 30 (7) (2005) 769 – 784. doi:10.1016/j.ijhydene.2004.08.001.

[12] T. Ekbom, M. Lindblom, N. Berglin, P. Ahlvik, Technical and commercial feasibility study of black liquor gasification with methanol/DME production as motor fuels for automotive uses - BLGMF, Tech. Rep. Contract No. 4.1030/Z/01-087/2001, Nykomb Synergetics (2003).

[13] V. Wan, Methanol to olefins, Report no. 261, SRI Consulting (2007).

[14] L. Fagernäs, J. Brammer, C. Wilen, M. Lauer, F. Verhoeff, Drying of biomass for second generation synfuel production, Biomass and Bioenergy 34 (9) (2010) 1267–1277.

[15] A. Rautalin, C. Wil Feeding biomass into pressure and related safety engineering, Research notes 1428, VTT, Laboratory of Fuel and Process Technology (1992).
URL http://bit.ly/1KkimVQ

[16] J. Brammer, A. Bridgwater, Drying technologies for an integrated gasification bio-energy plant, Renewable and Sustainable Energy Reviews 3 (4) (1999) 243 – 289.

[17] Metso brochure on KUVO belt dryer, Accessed July 8, 2013. [link].
URL http://bit.ly/10IwPme

[18] F. Lau, D. Bowen, R. Dihu, S. Doong, E. Hughes, R. Remick, R. Slimane, S. Turn, R. Zabransky, Techno-economic analysis of hydrogen production by gasification of biomass: Appendix B - Identification / Evaluation of solids handling systems, Final technical report under DOE contract number: DE-FC36-01GO11089, Gas Technology Institute (2002).

[19] E. Kurkela, Formation and removal of biomass-derived contaminants in fluidized-bed gasification processes, VTT Publications Vol.287, Technical Research Centre of Finland, VTT (1996).

[20] E. Kurkela, A. Moilanen, K. Kangasmaa, Gasification of biomass in a fluidised bed containing anti-agglomerating bed material, patent WO 00/011115 (2003).

[21] E. Kurkela, P. Ståhlberg, J. Laatikainen, Pressurized fluidized-bed gasification experiments with wood, peat and coal at VTT [Espoo, Finland] in 1991-1992, Part 1: Test facilities and gasification experiments with sawdust, VTT Publications 161, Technical Research Centre of Finland, VTT (1993).

[22] E. Kurkela, P. Ståhlberg, J. Laatikainen, P. Simell, Development of simplified IGCC-processes for biofuels: Supporting gasification research at VTT, Bioresource Technology 46 (1-2) (1993) 37–47, Power Production from Biomass.

[23] E. Simeone, M. Nacken, W. Haag, S. Heidenreich, W. de Jong, Filtration performance at high temperatures and analysis of ceramic filter elements during biomass gasification, Biomass and Bioenergy 35, Supplement 1 (0) (2011) S87 – S104, CHRISGAS. doi:10.1016/j.biombioe.2011.04.036.

[24] E. Simeone, M. Siedlecki, M. Nacken, S. Heidenreich, W. de Jong, High temperature gas filtration with ceramic candles and ashes characterisation during steam-oxygen blown gasification of biomass, Fuel 108 (0) (2013) 99 – 111. doi:10.1016/j.fuel.2011.10.030.

[25] E. Kurkela, P. Ståhlberg, J. Laatikainen, M. Nieminen, Removal of particulates and alkali-metals from the product gas of a pressurized fluid-bed gasifier, Proc. Int. Filtration & Separation Conf. Filtech Europa 1991, Karlsruhe, Germany (1991).

[26] M. Nieminen, E. Kurkela, Filtration of biomass and waste-derived gasification product gas, in: A. Bridgwater, D. Boocock (Eds.), Science in Thermal and Chemical Biomass Conversion, CPL Press, 2006, pp. 788–798.

[27] M. Nieminen, K. Kangasmaa, E. Kurkela, P. Ståhlberg, Durability of metal filters in low sulphur gasification gas, in: 3rd Symposium and Exhibition Gas Cleaning at High Temperatures, Karlsruhe, Germany, 1996, pp. 120–131.

[28] M. Nieminen, P. Simell, J. Leppälahti, P. Ståhlberg, E. Kurkela, High temperature cleaning of biomass-derived fuel gas, in: Proceedings of the 9th European Bioenergy Conference, Copenhagen, Denmark, 1996, pp. 1080–1086.

[29] T. Eriksson, J. Isaksson, P. Ståhlberg, E. Kurkela, V. Helanti, Durability of ceramic filters in hot gas filtration, Bioresource Technology 46 (12) (1993) 103 – 112, Power Production from Biomass. doi:10.1016/0960-8524(93)90060-O.

[30] E. Kurkela, P. Ståhlberg, J. Laatikainen, Pressurized fluidized-bed gasification experiments with wood, peat and coal at VTT in 1991-1994, Part 2: Experiences from peat and coal gasification and hot gas filtration, VTT Publications 249, Technical Research Centre of Finland (1995).

[31] L. Ma, H. Verelst, G. Baron, Integrated high temperature gas cleaning: Tar removal in biomass gasification with a catalytic filter, Catalysis Today 105 (34) (2005) 729 – 734, 2nd International Conference on Structured Catalysts and Reactors. doi:10.1016/j.cattod.2005.06.022.

[32] M. Nacken, L. Ma, S. Heidenreich, G. V. Baron, Performance of a catalytically activated ceramic hot gas filter for catalytic tar removal from biomass gasification gas, Applied Catalysis B: Environmental 88 (34) (2009) 292 – 298. doi:10.1016/j.apcatb.2008.11.011.

[33] M. Nacken, L. Ma, S. Heidenreich, F. Verpoort, G. V. Baron, Development of a catalytic ceramic foam for efficient tar reforming of a catalytic filter for hot gas cleaning of biomass-derived syngas, Applied Catalysis B: Environmental 125 (0) (2012) 111 – 119. doi:10.1016/j.apcatb.2012.05.027.

[34] M. Nacken, L. Ma, S. Heidenreich, G. V. Baron, Catalytic activity in naphthalene reforming of two types of catalytic filters for hot gas cleaning of biomass-derived syngas, Industrial & Engineering Chemistry Research 49 (12) (2010) 5536–5542. doi:10.1021/ie901428b.

[35] M. Nacken, L. Ma, K. Engelen, S. Heidenreich, G. V. Baron, Development of a tar reforming catalyst for integration in a ceramic filter element and use in hot gas cleaning, Industrial & Engineering Chemistry Research 46 (7) (2007) 1945–1951. doi:10.1021/ie060887t.

[36] E. Simeone, E. Holsken, M. Nacken, Study of the behaviour of a catalytic ceramic candle filter in a lab-scale unit at high temperatures, International Journal of Chemical Reactor Engineering 8 (2010) 1–19.

[37] K. Engelen, Y. Zhang, G. Baron, Development of a catalytic candle filter for one-step tar and particle removal in biomass gasification gas, International Journal of Chemical Reactor Engineeringdoi:10.2202/1542-6580.1062.

[38] L. Ma, G. V. Baron, Mixed zirconia-alumina supports for Ni/MgO based catalytic filters for biomass fuel gas cleaning, Powder Technology 180 (1-2) (2008) 21 – 29, papers presented at the 6th International Symposium on Gas Cleaning at High Temperature, Osaka, Japan 20-22 October 2005. doi:10.1016/j.powtec.2007.02.035.

[39] D. J. Draelants, H. Zhao, G. V. Baron, Preparation of catalytic filters by the urea method and its application for benzene cracking in $H_2S$-containing biomass gasification gas, Industrial & Engineering Chemistry Research 40 (15) (2001) 3309–3316. doi:10.1021/ie0009785.

[40] Y. Zhang, D. J. Draelants, K. Engelen, G. V. Baron, Development of nickel-activated catalytic filters for tar removal in $H_2S$-containing biomass gasification gas, Journal of Chemical Technology & Biotechnology 78 (2-3) (2003) 265–268. doi:10.1002/jctb.767.

[41] H. Zhao, D. J. Draelants, G. V. Baron, Performance of a nickel-activated candle filter for naphthalene cracking in synthetic biomass gasification gas, Industrial & Engineering Chemistry Research 39 (9) (2000) 3195–3201. doi:10.1021/ie000213x.

[42] K. Engelen, Y. Zhang, D. J. Draelants, G. V. Baron, A novel catalytic filter for tar removal from biomass gasification gas: Improvement of the catalytic activity in presence of $H_2S$, Chemical Engineering Science 58 (36) (2003) 665 – 670, 17th International Symposium of Chemical Reaction Engineering. doi:10.1016/S0009-2509(02)00593-6.

[43] F. Kirnbauer, V. Wilk, H. Hofbauer, Performance improvement of dual fluidized bed gasifiers by temperature reduction: The behavior of tar species in the product gas, Fuel 108 (0) (2013) 534 – 542. doi:10.1016/j.fuel.2012.11.065.

[44] L. Rabou, R. Zwart, B. Vreugdenhil, L. Bos, Tar in biomass producer gas, the Energy Research Centre of the Netherlands (ECN) experience: An enduring challenge, Energy & Fuels 23 (12) (2009) 6189–6198. doi:10.1021/ef9007032.

[45] Z. Abu El-Rub, E. A. Bramer, G. Brem, Review of catalysts for tar elimination in biomass gasification processes, Industrial & Engineering Chemistry Research 43 (22) (2004) 6911–6919. doi:10.1021/ie0498403.

[46] S. Anis, Z. Zainal, Tar reduction in biomass producer gas via mechanical, catalytic and thermal methods: A review, Renewable and Sustainable Energy Reviews 15 (5) (2011) 2355 – 2377. doi:10.1016/j.rser.2011.02.018.

[47] D. Dayton, A review of the literature on catalytic biomass tar destruction, milestone completion report NREL/TP-510-32815, National Renewable Energy Laboratory (2002).

[48] Y. Shen, K. Yoshikawa, Recent progresses in catalytic tar elimination during biomass gasification or pyrolysis - A review, Renewable and Sustainable Energy Reviews 21 (0) (2013) 371 – 392. doi:10.1016/j.rser.2012.12.062.

[49] C. C. Xu, J. Donald, E. Byambajav, Y. Ohtsuka, Recent advances in catalysts for hot-gas removal of tar and $NH_3$ from biomass gasification, Fuel 89 (8) (2010) 1784 – 1795. doi:10.1016/j.fuel.2010.02.014.

[50] M. M. Yung, W. S. Jablonski, K. A. Magrini-Bair, Review of catalytic conditioning of biomass-derived syngas, Energy & Fuels 23 (4) (2009) 1874–1887. doi:10.1021/ef800830n.

[51] Gasification of biomass is a success, Tech. rep., AAEN A/S, retrieved Dec 7th 2014 (2011). URL http://bit.ly/1BqIAkm

[52] I. Hannula, K. Lappi, P. Simell, E. Kurkela, P. Luoma, I. Haavisto, High efficiency biomass to power - operation experiences and economical aspects of the novel gasification process, in: 5th European Biomass Conference and Exhibition, from Research to Market Deployment, Berlin, 2007.

[53] S. Toppinen, I. Eilos, P. Simell, E. Kurkela, I. Hiltunen, Method of reforming gasification gas, Patent application US 2013/0058855 A1 (2012).

[54] P. Simell, E. Kurkela, Multiple stage method of reforming a gas containing tarry impurities employing a zirconium-based catalyst, Granted patent US 8100995 B2 (2012).

[55] P. Simell, E. Kurkela, Method for the purification of gasification gas, Granted patent US7455705 B2 (2008).

[56] S. J. Juutilainen, P. A. Simell, A. O. I. Krause, Zirconia: Selective oxidation catalyst for removal of tar and ammonia from biomass gasification gas, Applied Catalysis B: Environmental 62 (12) (2006) 86 – 92. doi:10.1016/j.apcatb.2005.05.009.

[57] H. Rönkkönen, E. Rikkinen, J. Linnekoski, P. Simell, M. Reinikainen, O. Krause, Effect of gasification gas components on naphthalene decomposition over $ZrO_2$, Catalysis Today 147, Supplement (0) (2009) S230 – S236, 3rd International Conference on Structured Catalysts and Reactors, ICOSCAR-3, Ischia, Italy, 27-30 September 2009. doi:10.1016/j.cattod.2009.07.044.

[58] H. Rönkkönen, P. Simell, M. Reinikainen, O. Krause, The effect of sulfur on $ZrO_2$-based biomass gasification gas clean-up catalysts, Topics in Catalysis 52 (8) (2009) 1070–1078. doi:10.1007/s11244-009-9255-8.

[59] W. Kaltner, Clariant/Sd-Chemie AG, Personal communication (July 2012).

[60] E. Supp, How to produce methanol from coal, Springer-Verlag, Berlin, Heidelberg, 1990.

[61] A. Kohl, R. Nielsen, Gas Purification (5th Edition), Elsevier, 1997.

[62] H. Weiss, Rectisol wash for purification of partial oxidation gases, Gas Sep Pur 2 (4) (1988) 171–176.

[63] Feed purification catalysts, Brochure, Haldor Topsøe A/S (2013).
URL http://bit.ly/17MQUqF

[64] P. Sabatier, J. Senderens, Nouvelles syntheses du methane, Acad Sci 314 (1902) 514–6.

[65] J. Kopyscinski, T. J. Schildhauer, S. M. Biollaz, Production of synthetic natural gas (SNG) from coal and dry biomass - A technology review from 1950 to 2009, Fuel 89 (8) (2010) 1763 – 1783.

[66] Practical experience gained during the first twenty years of operation of the great plains gasification plant and implications for future project, Tech. rep., U.S. Department of Energy (2006).

[67] M. Hedenskog, Gasification of forest residues - IRL in a large demonstration scale, Presentation at IEA biomass gasification workshop in Karlsruhe, Gteborg Energi (2014).
URL http://bit.ly/1OmgA4p

[68] T. Nguyen, L. Wissing, M. Skjth-Rasmussen, High temperature methanation: Catalyst considerations, Catalysis Today 215 (0) (2013) 233 – 238, Catalysis and synthetic fuels: state of the art and outlook. doi:10.1016/j.cattod.2013.03.035.

[69] From solid fuels to substitute natural gas (SNG) using TREMP, Tech. rep., Haldor Topsøe (2009).

[70] P. Huguen, G. Le Saux, Perspectives for a European standard on biomethane: a Biogasmax proposal, Project supported by the European Commission under RTD contract: 019795 (2010).
URL http://biogasmax.eu/

[71] M. Patart, French patent 540 343 (1921).

[72] P. Tijm, F. Waller, D. Brown, Methanol technology developments for the new millennium, Applied Catalysis A: General 221 (1-2) (2001) 275–282, Hoelderich Special Issue. doi:10.1016/S0926-860X(01)00805-5.

[73] M. Appl, Ammonia, Methanol, Hydrogen, Carbon Monoxide - Modern Production Technologies, Nitrogen, 1997.

[74] K. Mansfield, ICI experience in methanol, Nitrogen 221 (27).

[75] J.-P. Lange, Methanol synthesis: a short review of technology improvements, Catalysis Today 64 (1-2) (2001) 3–8.

[76] J. Ott, V. Gronemann, F. Pontzen, E. Fiedler, G. Grossmann, D. Kersebohm, G. Weiss, C. Witte, Methanol, in: Ullmann's Encyclopedia of Industrial Chemistry, Wiley-VCH Verlag GmbH & Co, 2012.

[77] Converter options for methanol synthesis, Nitrogen 210 (1994) 36–44.

[78] J. B. Hansen, P. E. Hojlund Nielsen, Methanol synthesis, in: Handbook of Heterogeneous Catalysis, Wiley-VCH Verlag GmbH & Co. KGaA, 2008. doi:10.1002/9783527610044.hetcat0148.

[79] R. Katofsky, The production of fluid fuels from biomass, CEES Rpt 279, Center for Energy and Environmental Studies, Princeton University (1993).

[80] H. Renon, J. M. Prausnitz, Local compositions in thermodynamic excess functions for liquid mixtures, AIChE Journal 14 (1) (1968) 135–144.

[81] C. D. Chang, A. J. Silvestri, The conversion of methanol and other O-compounds to hydrocarbons over zeolite catalysts, Journal of Catalysis 47 (2) (1977) 249–259.

[82] C. Chang, Hydrocarbons from methanol, Catal.Rev. 25 (1) (1983) 1–118.

[83] Wiley Critical Content - Petroleum Technology, Vol.1-2, John Wiley & Sons, 2007.

[84] S. Yurchak, Development of Mobil's fixed-bed methanol-to-gasoline (MTG) process, Stud.Surf.Sci.Catal. 36 (1988) 251–272.

[85] P. Nielsen, F. Joensen, J. Hansen, E. Sø rensen, J. Madsen, R. Mabrouk, Process for the preparation of hydrocarbons from oxygenates, Patent US 8067474 B2, Haldor Topsøe A/S (2011).

[86] E. Jorn, J. Rostrup-Nielsen, Process for the preparation of hydrocarbons, Patent US 4481305, Haldor Topsøe A/S (1984).

[87] F. Joensen, B. Voss, N. Schiø dt, Process to conversion of oxygenates to gasoline, patent US 8202413 B2, Haldor Topsøe A/S (2012).

[88] F. Joensen, B. Voss, J. Nerlov, Process for converting difficulty convertible oxygenates to gasoline, U.S. patent, Haldor Topsøe A/S (2010).

[89] A. Kam, M. Schreiner, S. Yurchak, Mobil methanol-to-gasoline process, in: Handbook of Synfuels Technology, R.A. Meyers (ed.), McGraw-Hill, 1984.

[90] J. Penick, W. Lee, J. Maziuk, Development of the methanol-to-gasoline process, in: Chemical Reaction Engineering - Plenary Lectures, ACS Symposium Series, Vol. 226, 1983, Ch. 3, pp. 19–48.

[91] J. Topp-Jø rgensen, Topsøe integrated gasoline synthesis - the tigas process, Stud.Surf.Sci.Catal. 36 (1988) 293–305.

[92] G. Soave, Equilibrium constants from a modified Redlich-Kwong equation of state, Chemical Engineering Science 27 (6) (1972) 1197 – 1203.

[93] E. Barker, J. Begovich, J. Clinton, P. Johnson, Aspen modeling of the tri-state indirect liquefaction process, contract no. W-7405-eng-6, Oak Ridge National Laboratory (1983).

[94] M. Schreiner, Research guidance studies to assess gasoline from coal by methanol-to-gasoline and sasol-type Fischer-Tropsch technologies, Final report to doe under contract no. ef-77-c-01-2447 (1978).

[95] A. Horvath, Carbona/Andritz, Personal communication (2012).

[96] R. Kallio, -consult, Personal communication (October 2012).

[97] S. Rackley, Carbon Capture and Storage, Elsevier, 2010.

[98] L. Bertuccioli, A. Chan, D. Hart, F. Lehner, B. Madden, E. Standen, Study on development of water electrolysis in the EU, Fuel cells and hydrogen joint undertaking (2014).

[99] J. Holladay, J. Hu, D. King, Y. Wang, An overview of hydrogen production technologies, Catalysis Today 139 (4) (2009) 244 – 260, Hydrogen Production - Selected papers from the Hydrogen Production Symposium at the American Chemical Society 234th National Meeting & Exposition, August 19-23, 2007, Boston, MA, USA. doi:10.1016/j.cattod.2008.08.039.

[100] J. Turner, G. Sverdrup, M. K. Mann, P.-C. Maness, B. Kroposki, M. Ghirardi, R. J. Evans, D. Blake, Renewable hydrogen production, International Journal of Energy Research 32 (5) (2008) 379–407. doi:10.1002/er.1372.

[101] J. Ivy, Summary of electrolytic hydrogen production - Milestone completion report, Tech. Rep. NREL/MP-560-36734, National Renewable Energy Laboratory (2004).

[102] C. Song, Global challenges and strategies for control, conversion and utilization of $CO_2$ for sustainable development involving energy, catalysis, adsorption and chemical processing, Catalysis Today 115 (1-4) (2006) 2–32.

[103] S. Saeidi, N. A. S. Amin, M. R. Rahimpour, Hydrogenation of $CO_2$ to value-added products - A review and potential future developments, Journal of $CO_2$ Utilization 5 (0) (2014) 66 – 81. doi:10.1016/j.jcou.2013.12.005.

[104] T. Inui, T. Takeguchi, Effective conversion of carbon dioxide and hydrogen to hydrocarbons, Catalysis Today 10 (1) (1991) 95 – 106. doi:10.1016/0920-5861(91)80077-M.

[105] T. Inui, K. Kitagawa, T. Takeguchi, T. Hagiwara, Y. Makino, Hydrogenation of carbon dioxide to $C_1$-$C_7$ hydrocarbons via methanol on composite catalysts, Applied Catalysis A: General 94 (1) (1993) 31 – 44. doi:10.1016/0926-860X(93)80043-P.

[106] M. Sahibzada, D. Chadwick, I. Metcalfe, Hydrogenation of carbon dioxide to methanol over palladium-promoted Cu/ZnO/$A1_2O_3$ catalysts, Catalysis Today 29 (14) (1996) 367 – 372, second Japan-EC Joint Workshop on the Frontiers of Catalytic Science and Technology for Energy, Environment and Risk Prevention. doi:10.1016/0920-5861(95)00306-1.

[107] K. Ushikoshi, K. Moria, T. Watanabe, M. Takeuchi, M. Saito, A 50 kg/day class test plant for methanol synthesis from $CO_2$ and $H_2$, in: T. Inui, M. Anpo, K. Izui, S. Yanagida, T. Yamaguchi

(Eds.), Advances in Chemical Conversions for Mitigating Carbon Dioxide Proceedings of the Fourth International Conference on Carbon Dioxide Utilization, Vol. 114 of Studies in Surface Science and Catalysis, Elsevier, 1998, pp. 357 – 362. doi:10.1016/S0167-2991(98)80770-2.

[108] M. Saito, R&D activities in Japan on methanol synthesis from $CO_2$ and $H_2$, Catalysis Surveys from Japan 2 (2) (1998) 175–184.

[109] D. Mignard, C. Pritchard, On the use of electrolytic hydrogen from variable renewable energies for the enhanced conversion of biomass to fuels, Chemical Engineering Research and Design 86 (5) (2008) 473 – 487. doi:10.1016/j.cherd.2007.12.008.

[110] T. Inui, Highly effective conversion of carbon dioxide to valuable compounds on composite catalysts, Catalysis Today 29 (14) (1996) 329 – 337, Second Japan-EC Joint Workshop on the Frontiers of Catalytic Science and Technology for Energy, Environment and Risk Prevention. doi:10.1016/0920-5861(95)00300-2.

[111] Y. Amenomiya, Methanol synthesis from $CO_2 + H_2$ II. Copper-based binary and ternary catalysts, Applied Catalysis 30 (1) (1987) 57 – 68. doi:10.1016/S0166-9834(00)81011-8.

[112] J. Graciani, K. Mudiyanselage, F. Xu, A. E. Baber, J. Evans, S. D. Senanayake, D. J. Stacchiola, P. Liu, J. Hrbek, J. F. Sanz, J. A. Rodriguez, Highly active copper-ceria and copper-ceria-titania catalysts for methanol synthesis from $CO_2$, Science 345 (6196) (2014) 546–550. doi:10.1126/science.1253057.